Contribution of Wave Setup to Projected Coastal Sea Level Changes

Melet A, Almar R, Hemer M, Gonéri Le Cozannet, Benoit Meyssignac, Ruggiero P

JGR Oceans

RESEARCH ARTICLE
10.1029/2020JC016078

Contribution of Wave Setup to Projected Coastal Sea Level Changes

A. Melet[1], R. Almar[2], M. Hemer[3], G. Le Cozannet[4], B. Meyssignac[2], and P. Ruggiero[5]

[1]Mercator Ocean International, Ramonville-Saint-Agne, France, [2]LEGOS, Université de Toulouse, CNES, CNRS, IRD, UPS, Toulouse, France, [3]Oceans and Atmosphere, CSIRO, Hobart, Tasmania, Australia, [4]BRGM/French Geological Survey, Orléans, France, [5]College of Earth, Ocean, and Atmospheric Sciences, Oregon State University, Corvallis, OR, USA

Key Points:
- Projected 20-yr mean wave setup changes are small but can attenuate or amplify total coastal sea level changes for the 21st century
- Wave setup can locally be a substantial contributor to departures of coastal sea level changes from global mean sea level rise
- Projected 20-yr mean wave runup changes can be large contributors to local departures from global mean sea level rise

Correspondence to:
A. Melet,
amelet@mercator-ocean.fr

Citation:
Melet, A., Almar, R., Hemer, M., Le Cozannet, G., Meyssignac, B., & Ruggiero, P. (2020). Contribution of wave setup to projected coastal sea level changes. *Journal of Geophysical Research: Oceans*, *125*, e2020JC016078. https://doi.org/10.1029/2020JC016078

Received 2 MAR 2020
Accepted 5 MAY 2020
Accepted article online 9 MAY 2020

Abstract Along open coasts, wind waves are a key driver of coastal changes and can be major contributors to coastal hazards. Wind wave characteristics are projected to change in response to climate change, notably due to changes in atmospheric circulation patterns and the associated surface winds. Here, a first-order estimate of projected 20-yr mean wave setup changes, excluding extreme events and subannual variability, is provided for sandy beaches along most of the world's coastline over the middle and end of the 21st century. Calculations are based on an ensemble of wave model projections under the representative concentration pathways (RCP) 8.5 and on empirical formulations for wave setup. Projected wave setup changes are compared to other contributors currently accounted for in regional sea level projections to extend existing projections of 21st century coastal sea level changes. Projected wave setup changes exhibit a clear spatial heterogeneity and mostly average out at global scale. However, at regional or local scale, wave setup changes are a small yet nonnegligible contributor to total coastal sea level 20-yr mean changes (which include global mean sea level rise, GMSLR) over the middle and end of the 21st century. Wave setup can be a substantial contributor to local departures of coastal sea level changes from GMSLR. Wave setup changes should therefore be included in projections of regional patterns of coastal sea level changes. The reported long-term changes in wave setup also advocate for the inclusion of nonstationary wave contributions to projected regional patterns of coastal sea level changes, including for studies on extreme events.

1. Introduction

Projected sea level (SL) changes are considered as a major threat for coastal zones (Cazenave & Le Cozannet, 2014; Hinkel et al., 2015), which are increasingly exposed to coastal erosion and flooding due to current and projected growth in coastal population, urbanization, and assets (Neumann et al., 2015).

SL changes at the coast result from processes acting at various space and time scales, from extreme events to long-term SL rise, with the superimposition of global, regional, and more local variations (e.g., Woodworth et al., 2019). As detailed hereafter, these various processes are typically not all accounted for in many SL studies. Rather, the selection of processes depends on the spatial and time scale of interest for SL changes. On the one hand, process-based SL projections over the 21st century account for the processes causing global to regional SL changes (e.g., Carson et al., 2016; Church et al., 2013; Slangen et al., 2014), but not yet for processes which express themselves locally, mostly in coastal zones. On the other hand, local processes are included in studies focused on extreme coastal SLs at local scale. In this study, we investigate the contribution of wind waves to projected time mean (20-yr mean, excluding extreme events and subannual variability) SL changes at the coast in the middle and end of the 21st century, to extend existing global projections of coastal mean SL changes.

Global mean sea level rise (GMSLR) is a direct and major consequence of climate change: It is induced by the thermal expansion of the ocean, by the transfer of land ice mass to the ocean (through melting glaciers and ice sheets plus dynamical ice processes leading to ice sheets mass loss) and by changes in terrestrial water storage (Church et al., 2013).

Regional (i.e., scales of O(100–1,000 km)) SL changes can deviate from GMSLR, with spatial departures mostly ranging within ±30% of the global rise (Church et al., 2013; Slangen et al., 2014). Spatial variations

of SL changes at regional scale are due to the dynamical response of the ocean to the atmospheric forcing and the associated redistribution of ocean heat, salt, and mass (e.g., Forget & Ponte, 2015), to changes in atmospheric pressure loading induced by changes in the atmospheric circulation and moisture content (inverted barometer effect, e.g., Wunsch & Stammer, 1997), and to the solid Earth deformation and effects on the Earth's geoid (arising from both gravitational and rotational effects) associated with the transfer of water mass from land to the ocean (from glaciers, ice sheets, and terrestrial water, e.g., Slangen et al., 2014) and to the glacial isostatic adjustment (GIA, Peltier et al., 2015).

Global and regional SL projections based on the Climate Model Intercomparison Project Phase 5 (CMIP5, Taylor et al., 2012) account for the aforementioned processes (e.g., Church et al., 2013; Slangen et al., 2014). The ability of CMIP5 models to reproduce observed SL changes over the twentieth century has been assessed in Meyssignac et al. (2017) and Slangen et al. (2017).

At coastal scales, apart from natural or anthropogenic-induced local vertical land motion, several other processes lead to substantial SL changes from the open ocean and should be considered when estimating local SL changes at the coast (Woodworth et al., 2019). Among these processes are tides, atmospheric surges, and wind wave contributions. Wave contributions are due to both locally generated wind waves (wind sea waves) and remotely generated waves (swells) and can be decomposed into wave setup (time mean dynamic elevation of SL due to wave breaking) and swash (waterline oscillations at the time scale of individual waves and wave groups) (Dodet et al., 2019). Together, wave setup and swash combine to achieve the wave runup being the maximum elevation reached by the swash.

Wave-induced coastal SL changes can span time scales ranging from seconds to decades. Swash and runup vary at the wave phase resolved time scales and wave setup from phase-averaged to synoptic time scales (Dodet et al., 2019). The amplitude of wave contributions to coastal SL changes is much larger at very short time scales than at longer time scales. For this reason, waves have mostly been considered in local studies for their substantial contribution to extreme total water levels at open coasts (e.g., Hoeke et al., 2013; Pedreros et al., 2018; Stockdon et al., 2007; Wadey et al., 2017). Global-scale studies of past extreme water levels are often based on tide gauges. As tide gauges are typically located in wave-sheltered environments, wave contributions to SL extremes have been mostly unaccounted for until recently in global-scale coastal risk assessments (as recalled by Wahl et al., 2017). Regional- to global-scale studies accounting for wave contributions to past (e.g., Rueda et al., 2017; Ruggiero, 2013; Serafin et al., 2017; Vousdoukas et al., 2016) and projected extreme water levels at the coast are emerging (e.g., Arns et al., 2017; Mentaschi et al., 2017; Vitousek et al., 2017; Vousdoukas et al., 2017; Vousdoukas, Mentaschi, Voukouvalas, Verlaan, et al., 2018; Vousdoukas, Mentaschi, Voukouvalas, Bianchi, et al., 2018). They highlight the prominent role of wind waves in coastal hazards for low-lying coasts, contributing to coastal erosion and flooding via elevated total water levels and high-energy fluxes.

Wave setup can also exhibit low-frequency changes (e.g., Melet et al., 2016, 2018; Ponte et al., 2019; Woodworth et al., 2019) through its dependence on many factors that can change over long time scales (seasonal to multidecadal). These factors include (1) changes in geomorphology (e.g., beach orientation and nearshore bathymetry, Familkhalili & Talke, 2016; Lentz et al., 2016; Cohn & Ruggiero, 2016; Hongo et al., 2018), (2) changes in ocean currents, water depth (including SL rise), and their interaction with waves (e.g., Arns et al., 2017; Hoeke et al., 2015; Quilfen et al., 2018; Wandres et al., 2017), and (3) changes in deep-ocean wave characteristics (significant wave height, period, and direction) induced by changes in atmospheric circulation patterns and the consequent surface winds, in response to internal climate variability and climate change. Although there remain uncertainties regarding the robustness of externally forced trends in wave height and their extremes over the last decades (e.g., Semedo et al., 2011; Reguero et al., 2019; Young & Ribal, 2019; Dodet et al., 2019; Mori et al., 2019), robust changes in wave height, period, and direction are projected for the 21st century over several oceanic regions (e.g., Hemer et al., 2013; Morim et al., 2018, 2019; Wang et al., 2014). These low-frequency changes in wave climate are transmitted to total water level changes at the coast through wave setup and swash changes. However, few studies have focused on the seasonal, interannual, or longer-term changes of wave setup and swash. Apart from the fact that wave contributions are larger during extreme events, this might also be due to the lack of continuous long time series of wave setup and runup, due to limitations in observations (Dodet et al., 2019; Ponte et al., 2019) and in coastal numerical models for a realistic representation of nearshore morphological evolution

(Elsayed & Oumeraci, 2017). An exception is the study of Gainza et al. (2018) in which an interannual time series of wave runup was produced using a metamodeling approach. A complicating factor in studying low-frequency changes in wave setup and runup is also their sensitivity to poorly known time-varying local morphology (e.g., O'Grady et al., 2019). Yet, several studies have shown interannual variability of deep water wave energy flux, nearshore profile, shoreline position, and beach width and volume (e.g., Harley et al., 2017; Karunarathna et al., 2016; Kuriyama et al., 2012; Norcross et al., 2002). Recently, Melet et al. (2018) performed a global-scale, first-order estimate of the contribution of wave setup to past interannual-to-multidecadal changes in coastal total water levels. Their results pinpoint the sizable wind wave-induced contribution to interannual-to-multidecadal total water level changes over the past two decades and suggest that wave contributions should not only be considered for extreme events studies but should also be included in studies of past and future low-frequency coastal SL changes and rise.

The present study aims at giving a first-order global estimate of the importance of wave contributions to 20-yr mean coastal SL changes due to changing winds during the 21st century and to compare them to the other SL contributions that are currently accounted for in regional mean SL projections (e.g., Carson et al., 2016; Church et al., 2013; Oppenheimer et al., 2019). Changes in mean SLs can lead to various impacts, such as an increase in frequency of extreme water levels at the coast, degradation of coastal ecosystems, salinization of surface and groundwater, or permanent flooding (Oppenheimer et al., 2019). A better understanding of the drivers of coastal SL changes is indeed a prerequisite for reliable projections of SL changes at the coast, which are needed to assess the vulnerability of the coastline and to quantify adaptation needs (e.g., Bouwer, 2018; Hallegate et al., 2013; Hinkel et al., 2014).

We mostly focus on wave setup changes on sandy beach environments. Sandy beaches are ubiquitous along the world's coastlines (Luijendijk et al., 2018), can represent the first line of defense for flooding, and are among the most vulnerable coastal environment to SL rise (Wong et al., 2014). We mostly focus on wave setup changes, as they contribute to time mean SL changes and are more directly comparable to other contributors in current SL change projections. Yet wave runup changes and implications of our results for other coastal environments are discussed in section 4.

2. Methods and Data

2.1. Regional SL Change Contributions

2.1.1. Contributions Accounted for in AR5

Contributions to relative SL changes accounted for in IPCC AR5 projections used here are based on the data sets used in Carson et al. (2016) and Slangen et al. (2014). A brief synthesis is provided below.

The ocean component includes steric effects—including the global mean thermal expansion of the ocean—and the dynamical ocean response and currents. SL changes due to atmospheric pressure loading (inverted barometer effect), associated with changes in atmospheric circulation and moisture content, are added to the ocean component. This ocean component (referred to as sterodynamic SL hereafter following Gregory et al., 2019) is directly computed from an ensemble of 21 CMIP5 climate models (Slangen et al., 2014). Glacier mass loss is computed from a global glacier model based on a volume-area approach (Slangen & van de Wal, 2011) and using CMIP5 projections of temperature and precipitation changes at glacier locations for each of the 21 climate models. Ice sheet surface mass balance contributions are computed using empirical relationships to global surface mean temperature change, which are provided by the 21 CMIP5 climate model projections. Dynamical mass loss of the ice sheets is constructed from two literature-based estimates: The lower estimate is provided by the scaled-up estimate of the IPCC AR4 (Meehl et al., 2007), which assumes continuation (with no acceleration) of 1993–2003 changes, while the upper estimate is given by Katsman (2011), who assumes a continued observed discharge in the Amundsen Sea Embayment and East Antarctica and retreating ice shelves near tidewater glaciers in Greenland. An average of the two is taken as the mean contribution. The deformation of the solid Earth and associated vertical land motions due to the last glacial maximum land ice melting (GIA) is computed from the ICE5G model (Peltier, 2004). Terrestrial water storage changes are estimated from Wada et al. (2012).

For contributors adding mass to the ocean (glaciers, ice sheets, and terrestrial groundwater), mass spatial redistribution over the ocean is computed accounting for gravitational, rotational, and viscoelastic deformation effects.

The dynamic ice sheet, terrestrial groundwater and GIA contributions are scenario-independent in the data set used in Slangen et al. (2014) and Carson et al. (2016). All other contributions are computed over the 21st century under a moderate-emission-mitigation-policy climate change scenario (representative concentration pathways, RCP4.5), and under a high emission RCP8.5 scenario. RCP4.5 and 8.5 lead to CO_2-equivalent concentrations reaching 650 ppm and more than 1,370 ppm respectively in 2100 (Moss et al., 2010).

Contributions to SL changes are relative to the 1986–2005 historical period used in AR5. All contributions are provided on 1° × 1° maps and as annual averages.

2.1.2. Wave Setup and Swash Contributions

Global-scale, long-term changes in wave setup (η) and runup ($R_{2\%}$) in response to climate change are predicted here for sandy beaches from the commonly used Stockdon et al. (2006) (S06 hereafter) generic empirical formulations:

$$\eta = 0.35\,\beta\sqrt{H_s L_p} \tag{1}$$

$$R_{2\%} = 1.1\left(0.35\beta\sqrt{H_s L_p} + 0.5\left[H_s L_p\left(0.5625\beta^2 + 0.004\right)\right]^{1/2}\right) \tag{2}$$

where $R_{2\%}$ is the 2% exceedance wave runup. In 1 and 2, β is the foreshore beach slope, H_s is the deep water wave height, and L_p is the deep water peak wave wavelength and is related to the deep water peak wave period T_p through the linear dispersion relationship:

$$L_p = \frac{g}{2\pi}T_p^2 \tag{3}$$

where g is the acceleration of gravity.

Time series of H_s and T_p are issued from an ensemble of global wave model projections (Hemer & Trenham, 2016), using 6-hourly significant wave height and peak wave period respectively. Hemer and Trenham (2016) ran the WaveWatchIII wave model on a near global domain at 1° × 1° spatial resolution forced by surface winds and sea ice concentration fields from eight CMIP5 climate models (ACCESS1.0, BCC-CSM1.1, CNRM-CM5, GFDL-CM3, HadGEM2-ES, INMCM4, MIROC5, and MRI-CGCM3) over the historical period (1986–2005), mid-21st century (2026–2045) and end of 21st century (2081–2100) using RCP4.5 and 8.5. The corresponding GCM forced wave model simulations were evaluated over the historical period in Hemer and Trenham (2016). Following their assessment, simulations forced with CNRM-CM5 were excluded from our analysis.

Wave setup and runup depend on the foreshore beach slope β (equations 1 and 2), which varies in time and in space. We consider different cases for β:

1. β_{lc}: Locally observed, time-invariant beach face slope. We used the data set of Barboza and Defeo (2015) and complemented it with a literature search (Almar et al., 2019; Bascom, 1951; Bujalesky, 2007; Carranza-Edwards et al., 1998; Carrasco et al., 2009; Cesaraccio et al., 2004; Cuevas et al., 2010; Díaz-Sánchez et al., 2014; Isla & Bujalesky, 2005; Ivamy & Kench, 2006; Karunarathna et al., 2016; Lefebvre et al., 2014; Maurer & Johnson, 2017; Norcross et al., 2002; Pino & Jaramillo, 1992; Poulos et al., 2013; Reis & Gama, 2009; Rodríguez-Polo et al., 2018; Sénéchal, 2017; S06). Foreshore beach slopes are provided for 308 beaches worldwide (Figure 1a), ranging from 0.005 to 0.20, with a median value of 0.04 and a mean value of 0.055.
2. β_{gc}: Globally constant, time-invariant beach face slope. We use a constant beach slope of 0.04, which corresponds to the median value of the 308 local beach slopes from Barboza and Defeo (2015).

Since beach morphology also evolves in time and influences wave setup and runup through a complex equilibration process, a number of studies have developed empirical relationships for predicting the equilibrium slope in terms of the wave steepness (H_s/L_p) (e.g., Madsen & Plant, 2001). To partly account for morphological feedbacks on wave setup and runup, we use the Sunamura (1984) formulation for computing time-varying beach face slopes:

$$\beta = 0.12\left[\frac{\sqrt{2\pi D_{50} L_p}}{H_s}\right]^{1/2}, \tag{4}$$

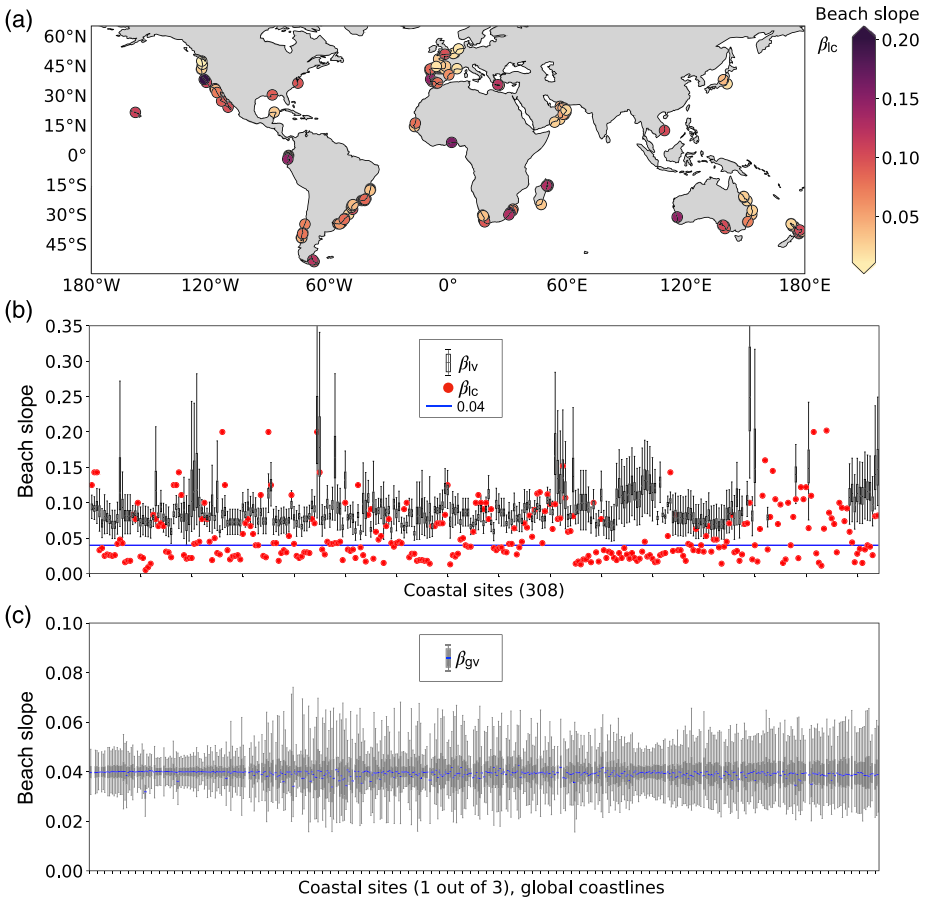

Figure 1. Beach face slopes. (a) Values of the reported 308 beach face slopes used for β_{lc}. (b, c) Distribution of the monthly mean time series of beach slope values β_{lv} in panel (b), β_{gv} in panel (c) computed using the outputs from the seven global wave models over the historical period 1986–2005. For each coastal site (along the x axis, 308 sites in (b), every third of the 1,521 sites along the global coastlines in (c)), the boxplot (y axis) represents the interquartile range IQR = Q3–Q1 (black rectangle) of the beach slope time series, and the range (Q1–1.5*IQR, Q3 + 1.5*IQR) (black vertical line) where Q1 and Q3 are, respectively, the 1st and 3rd quartiles of the beach slope distribution. In (b), the beach slope is computed using equation 4 and reported local values of the sediment grain sizes, with no capping or normalization (section 2.1.2). Red dots correspond to reported beach slopes shown in panel (a). The horizontal blue line corresponds to the median value of reported beach slopes of 0.04. In (c) beach slopes correspond to normalized β_{gv} along the world coastline (equatorward of 60°N/60°S (see section 2.1.2 for more details) and the blue lines correspond to the median value of the time-varying β_{gv}.

where D_{50} is the median diameter of the beach sand. This formulation lets the beach slope evolve with varying incoming wave conditions. When using equation 4 with reported local median diameter of sand grains (Barboza & Defeo, 2015) and the wave model ensemble 6-hourly H_s and L_p, the median of the predicted local time-varying beach slopes β_{lv} tends to be larger than observed beach slope for a large number of coastal sites (Figure 1b). Yet estimates of adaptative, time-varying beach slopes are useful to complement the static beach slope case and to provide a range of uncertainty. We therefore considered a third case for the beach slope:

3. β_{gv}: Global, time-varying beach face slope. β_{gv} is computed using equation 4 from 6-hourly H_s and L_p and a uniform, representative value for fine to medium-grained sand size of 250 μm for D_{50} (Rueda et al., 2017). The resulting 6-hourly beach slopes are then capped at 0.20 and scaled by a normalization factor to ensure that the time mean of the beach slope stays close to 0.04. In the remainder of the text and analysis, β_{gv} is normalized. The distribution of time-varying beach slopes β_{gv} is shown in Figure 1c. The time variability of the beach slope can be important at various coastal sites, with slopes

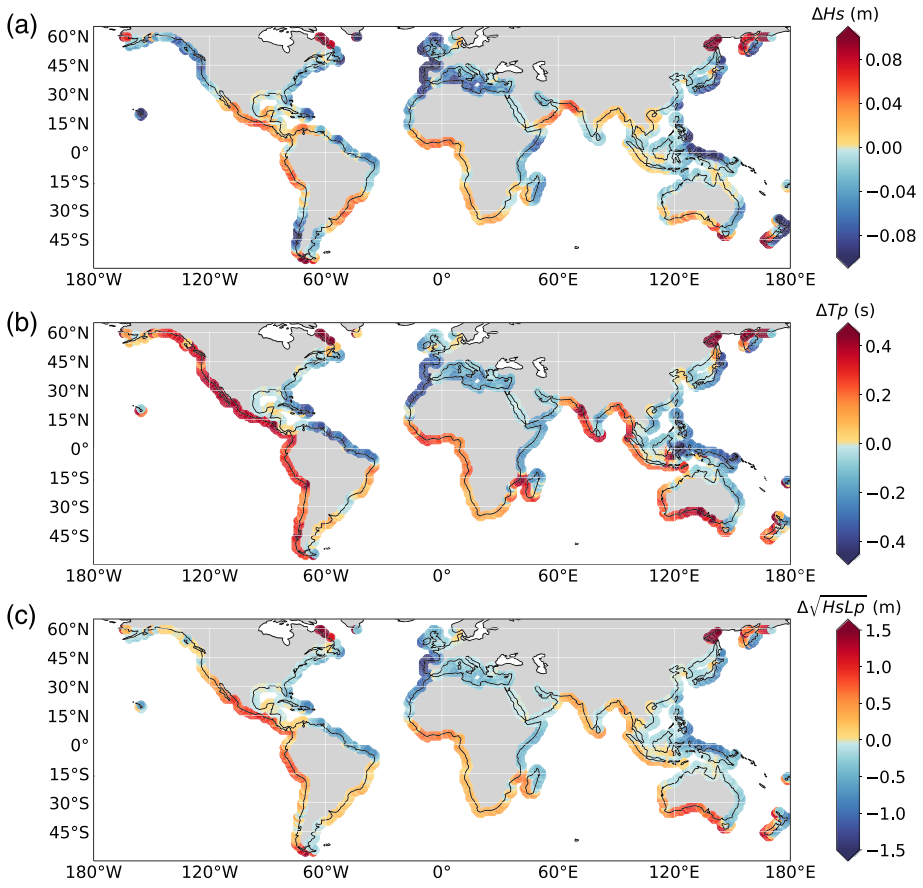

Figure 2. Projected changes in incoming wave conditions. Ensemble-mean projected changes from 1986–2005 to 2081–2100 under the RCP8.5 scenario in (a) significant wave height (ΔHs, in m), (b) peak period (ΔTp, in s), and (c) $\Delta\,(HsLp)^{0.5}$ (in m), a common scaling for wave setup (see section 4).

varying between roughly 0.015 and 0.08 (Figure 1c). Comparing estimates of wave setup and runup based on β_{gv} to those based on β_{gc} allows us to exploit the effect of time-varying beach slopes on wave contributions to total water levels at the coast.

Limitations on estimates of wave setup and runup using this methodology are discussed in section 4.

For each of the seven global wave models, wave setup and runup were computed from 6-hourly outputs of H_s and T_p. To extract the long-term changes in wave setup and runup, high frequencies were first excluded from our analysis as follows. We detrended the time series using a linear fit and then removed the seasonal cycle with a fit to a fourth-degree polynomial of 1-yr periodicity. We then low-pass filtered the resulting time series in frequency space based on a Hamming window with a cutoff period of 1.2 yr to exclude extreme events and other subannual changes. The trend was then added back, yearly means were computed and averaged to compute the three 20-yr periods considered here (1986–2005, 2026–2045, and 2081–2100). Finally, the time series were referenced to the historical 20-yr mean (1986–2005). Time series of the seven-member ensemble mean and standard deviation were computed.

2.2. Coastal Points

In addition to estimates at the 308 coastal sites for which reported beach slopes were used, we also provide estimates along the world's coastlines. As wave projections are masked by sea ice-covered areas, we restrict our analyses to coastal regions equatorward of 60°N/60°S (which encompass most of the heavily populated coastlines). Coastal points were selected from the coastal mask defined in Carson et al. (2016) (corresponding to grid cells on the 1° × 1° grid where at least one side bordered a land cell). There were 1,521 points selected (e.g., Figure 2). Wave projections are not provided on the

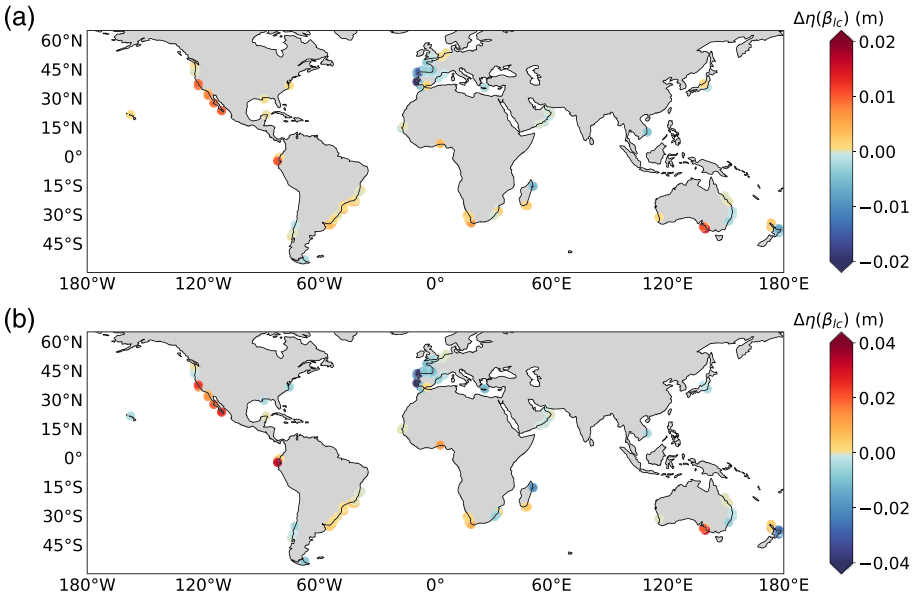

Figure 3. Projected wave setup changes using local beach slope estimates. Projected ensemble mean wave setup changes from 1986–2005 to (a) 2026–2045 and (b) 2081–2100 under the RCP8.5 scenario using local time-invariant beach face slopes β_{lc}. Units are in meters. Note the different color bars for the two periods.

same 1° × 1° grid as the Carson et al. (2016) data (grid offset of 0.042° in latitude and −0.042° in longitude in the wave model). The closest point in the wave model grid to the coastal point was selected for wave projections.

3. Results

The contribution of wave setup changes to 20-yr mean projected coastal SL changes from the reference historical period (1986–2005) is compared to the other contributions over the middle (2026–2045) and end of the 21st century (2081–2100). Two climate change scenarios were used RCP4.5 and RCP8.5, but results are shown for the RCP8.5 scenario only.

3.1. Projected Changes in Wave Conditions

Wave setup changes considered in our study arise from changes in wave height and period induced by changes in surface winds (equation 1). Thus, we first illustrate projected changes in the ensemble mean significant wave height, peak period and scaling $(HsLp)^{0.5}$ in Figure 2 for the end of the century. At large scales, model-ensemble projected changes are coherent with projected changes described in Hemer et al. (2013) and Morim et al. (2018, 2019). Projected changes are regionally consistent, with for instance a decrease in significant wave height and periods along the coastlines of western Europe and of the Mediterranean Sea. Changes in wave height and peak period result from changes in the different waves composing the wave spectra (waves generated at different locations and time), which can be of the same or opposite sign depending on regions, and therefore add up or partly compensate in the total wave height and period changes (Fan et al., 2014). For instance, the projected significant wave height decrease along the western coast of Europe (Figure 2a) is due to a decrease of both swell and wind sea wave heights (not shown). On the other hand, projected wave height increase along the southern coast of Australia is a combination of reduced wind sea wave heights and greater swell wave heights. Projected increased swell period over large portions of the western coasts of the continents in the Southern Hemisphere can be related to projected enhanced wave generation in the Southern Ocean and its extended influence on remote coastlines as corresponding swells propagate northward (Hemer et al., 2013).

3.2. Projected Changes in Wave Setup

Projected changes of the ensemble mean wave setup relative to the historical period are shown in Figure 3 for the 308 local sites. Wave setup changes induce positive or negative coastal SL changes of a few

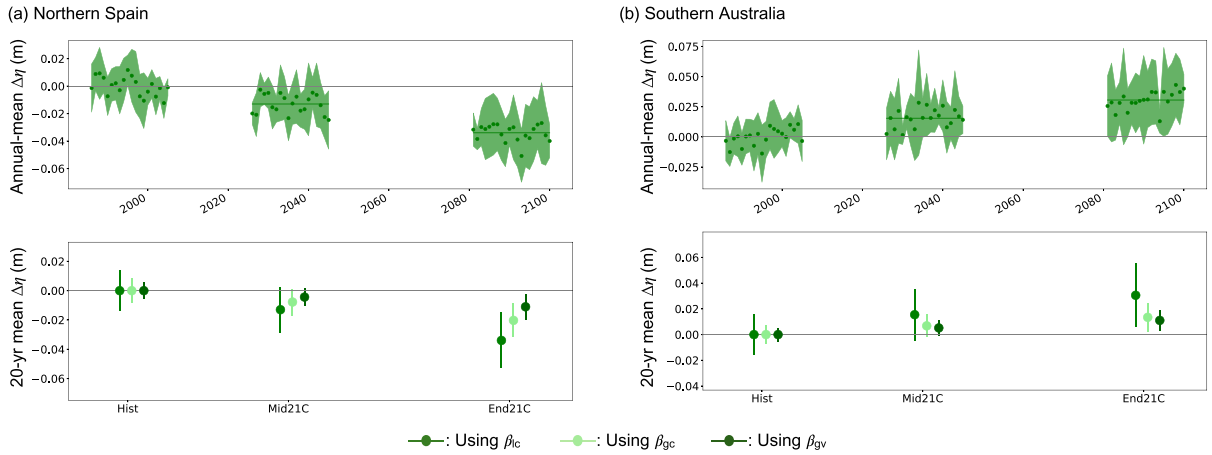

Figure 4. Local wave setup changes. Upper panels: time series of annual mean wave setup changes referenced to the 1986–2005 mean ($\Delta\eta$, in meters) under the RCP8.5 scenario and using a time-invariant local beach slope (β_{lc}) at coastal sites located (a) in Northern Spain ($\beta_{lc} = 0.067$) and (b) in Southern Australia ($\beta_{lc} = 0.09$). Dots show the seven-member ensemble mean, and shading the ensemble standard deviation. Horizontal green lines show the 20-yr mean changes. Lower panels: local comparisons of the 20-yr time mean wave setup changes ($\Delta\eta$, in meters) using different cases for the beach slope, that is, from left to right the local time-invariant beach slope β_{lc} (in green; corresponding to the horizontal lines in upper panels), the globally constant beach slope of 0.04 β_{gc} (light green), the time-varying beach slope β_{gv} (dark green). Circles correspond to the ensemble mean wave setup changes, vertical lines to the ensemble standard deviation.

centimeters in 2026–2045 and 2081–2100 (Figure 3), with changes of the same sign and of larger amplitude over 2081–2100 compared to 2026–2045. This is further illustrated in Figure 4 for two contrasted coastal sites (Northern Spain and Southern Australia) with annual mean time series of the ensemble mean wave setup changes relative to the 1986–2005 mean. Using a seven-member ensemble mean reduces the signature of internal climate variability on wave setup changes, as atmospheric forcing used to generate the wave-model ensemble are issued from coupled ocean-atmosphere CMIP models whose internal climate variability (which is made of weather events and climate modes) is unphased between each other. Yet the number of members in the ensemble is not large enough to completely remove the signature of interannual variability due to internal climate variability in the ensemble mean wave setup changes. Consistent with the results of O'Grady et al. (2019), who demonstrated that wave setup estimates for the coastlines of Australia are very sensitive to beach slope characteristics, the amplitude of wave setup changes depends on the choice of the foreshore beach slope. This is illustrated in Figure 4 with wave setup estimated with the locally reported slopes (β_{lc}, here 0.07 and 0.09, respectively, in Figures 4a and 4b), a time-invariant slope of 0.04 (β_{gc}), and a slope varying in time around 0.04 to adjust for varying wave conditions. Normalizing the beach slope to only account for the time variations of beach slope around a fixed time mean of 0.04 generally leads to lower contributions of waves to coastal SL changes than using a time-invariant beach slope of 0.04. This might be explained by the dynamical adjustment of the beach slope to incoming wave conditions: the beach slope flattens when waves are steeper (equation 3). This could lead to a partial compensation in wave setup when using the S06 formulation (equation 1). It should be clear however that the spatial variability of sediment grain size strongly influences the spatial variability of beach slopes. This effect is not accounted for in our global estimates as the time mean beach slope is set to 0.04 everywhere.

Global-scale estimates of projected wave setup changes exhibit a clear spatial heterogeneity but with regional-scale coherence (Figure 5) due to the regional coherence of offshore wave changes and the use of a uniform (β_{gc}) or regionally coherent (β_{gv}) beach slope. For instance, wave setup is projected to increase along the western coasts of North and South America, the western coast of southern Africa, the southern coast of Australia, the western coast of India, most of the eastern coasts of the Indian Ocean, and the western coast of New Zealand. On the contrary, wave setup is projected to decrease along the western coast of Europe and northwestern Africa, most of the Mediterranean coasts, the tropical and subtropical western Pacific coasts, the east coast of New Zealand, most of the west coasts of the Indian Ocean, and the western coasts of the Tropical Atlantic Ocean. The spatial distribution of projected changes is consistent between (i) the two 20-yr periods considered for the 21st century, but changes are larger at the end of the 21st century than for the mid-21st century (Figure 5), (ii) RCP8.5 and 4.5 (not shown), with greater amplitude in RCP8.5

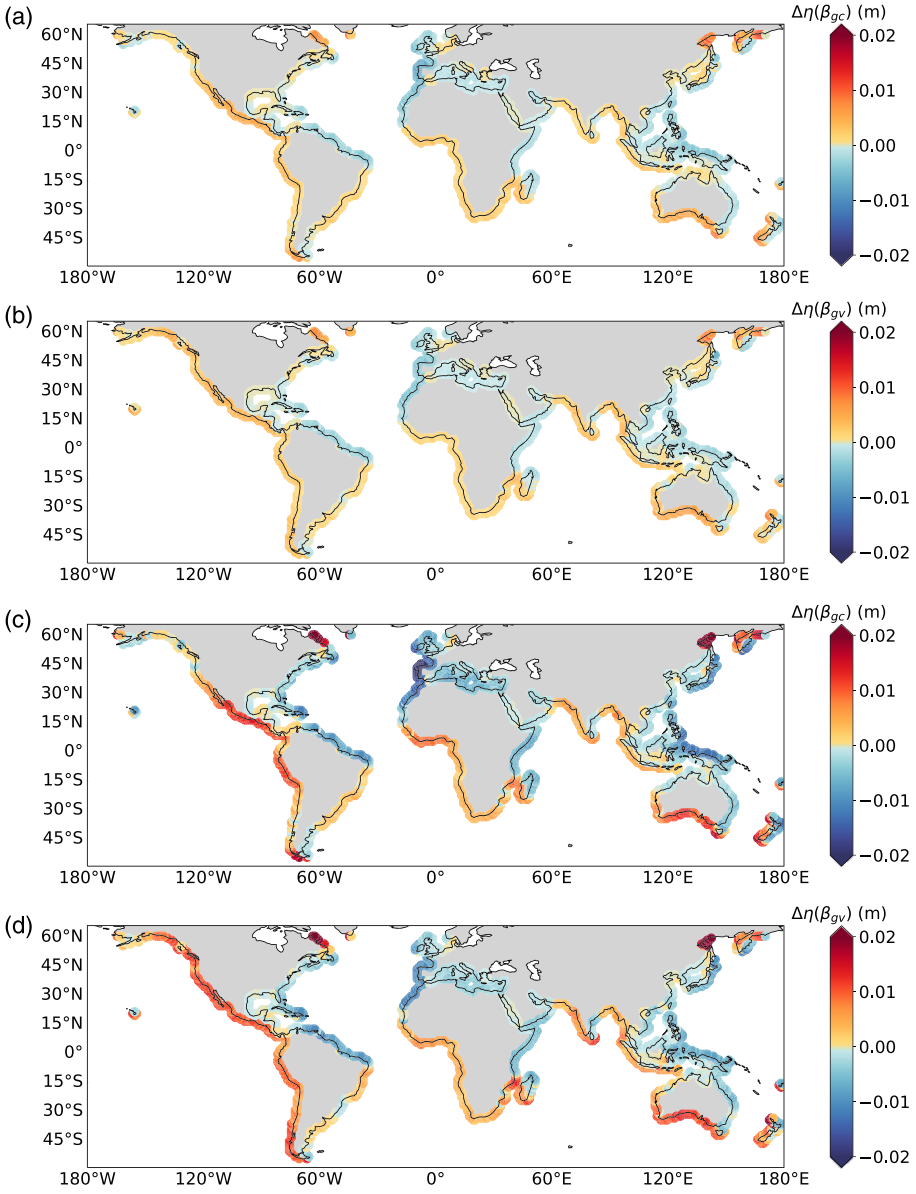

Figure 5. Projected wave setup changes at global scale. Projected ensemble mean wave setup changes from 1986–2005 to (a, b) 2026–2045 and (c, d) 2081–2100 under the RCP8.5 scenario, using (a, c) a time-invariant beach slope of 0.04 (β_{gc}) and (b, d) time-varying normalized beach slopes (β_{gv}). Units are in meters.

projections, and (iii) the different cases used for the beach slope (β_{gc} vs. β_{gv}), with very similar amplitudes of wave setup changes when the beach slope evolves in response to incoming wave conditions but has the same time mean value. The robustness in wave setup changes across periods and climate change scenarios suggests that projected wave setup changes shown in Figure 5 are mostly related to forced climate change. The ensemble mean wave setup changes exceeds the ensemble intermodel standard deviation of wave setup changes, especially in regions with the largest projected wave setup changes, and even more so over the 2081–2100 period (not shown). This is indicative of predominantly climate change driven changes, over large portions of the world's coastline. The distribution of these robust changes also broadly aligns with studies of projected changes in wave conditions (e.g., Hemer et al., 2013; Morim et al., 2018, 2019).

Projected changes in wave setup are a combination of projected changes in wind wave-induced setup and of swell-induced setup. Overall, projected changes in wave setup are more consistent with projected changes in

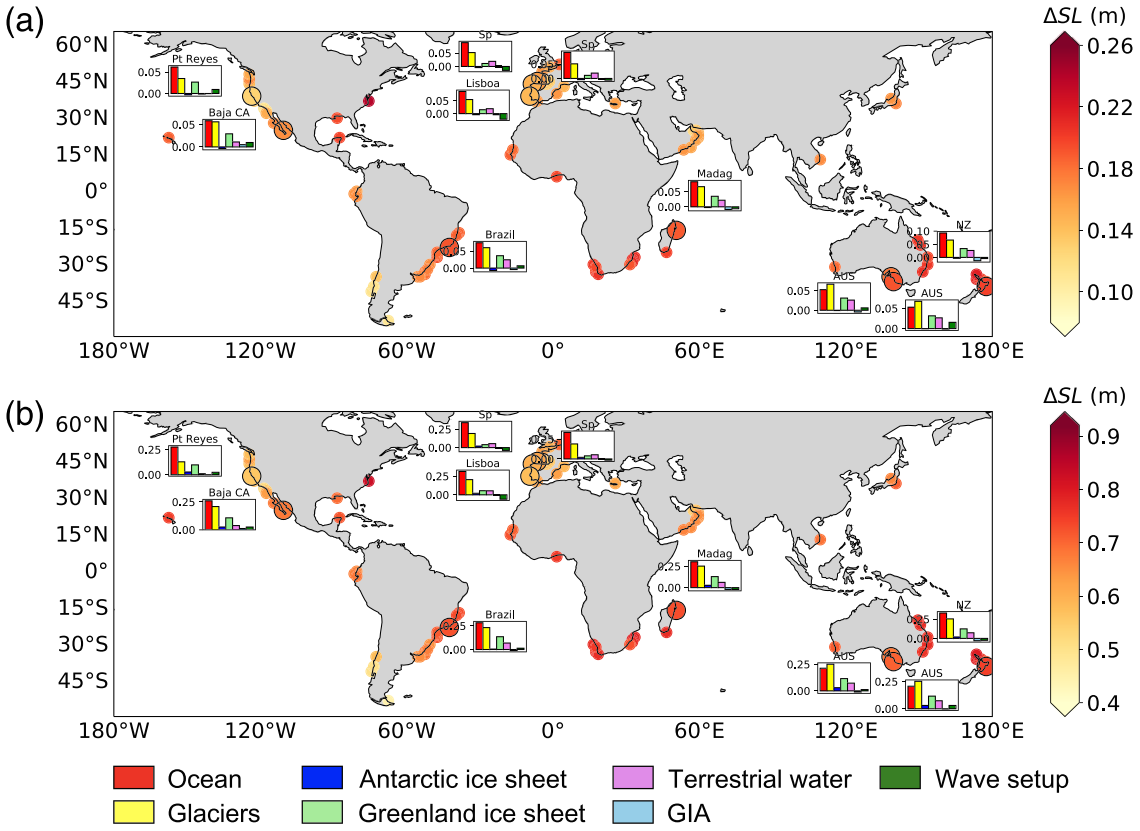

Figure 6. Contributions to projected coastal mean sea level changes. Projected coastal SL changes (ΔSL) (sum of sterodynamic SL, glaciers, Antarctic ice sheet, Greenland ice sheet, terrestrial water, GIA, wave setup) from 1986–2005 to (a) 2026–2045 and (b) 2081–2100 under RCP8.5, in meters. Wave setup was computed using local time-invariant beach slopes β_{lc}. Insets show the contribution of the different processes (legend at the bottom) to coastal SL changes at different coastal grid points (indicated by black circles). Units are in meters. Sp. stands for Spain, AUS for Australia, NZ for New Zealand, and Baja CA for Baja California.

swell-induced wave setup and in particular changes in wave period rather than in wave height, especially where swell contribution is large (e.g., western coast of North and South America and southern coast of Australia) (not shown).

3.3. Contribution of Wave Setup Changes to Coastal SL Changes

We now discuss the relative importance of projected wave setup changes compared to projected changes in other contributors to coastal SL over 20-yr means. Regional maps of projected changes of contributors other than wave setup used in the present study can be found in Slangen et al. (2014) over the global ocean. Projected coastal mean SL changes (including wave setup changes) are shown in Figure 6 for the 308 coastal sites together with the breakdown by components at several coastal locations with relatively sizable projected wave setup changes. At these coastal locations, wave setup change magnitudes are small yet relatively sizable compared to the main contributors of coastal SL changes, such as the sterodynamic SL or the glaciers mass loss. Wave setup changes can reach amplitudes similar to those induced by GIA or land water transfers (bar histograms in Figure 6). Projected wave setup changes at the end of the 21st century become slightly less important relative to changes in other contributors (Figure 6b), although they remain sizable over extended portions of the coastlines (Figure 5).

As an interesting feature of projected wave setup changes is their rather large spatial heterogeneity (Figures 4 and 5), global estimates of the spatial departure of each component of projected coastal SL change from its own global coastal mean value are shown in Figures 7a and 7b to update results from Carson et al. (2016) with the addition of the wave setup contribution. Breakdowns of projected spatial departures of coastal SL changes from GMSLR into its components are illustrated at several coastal sites. The selected sites in Figure 7 follow a subset of locations chosen in Carson et al. (2016) to span diverse coastal locations

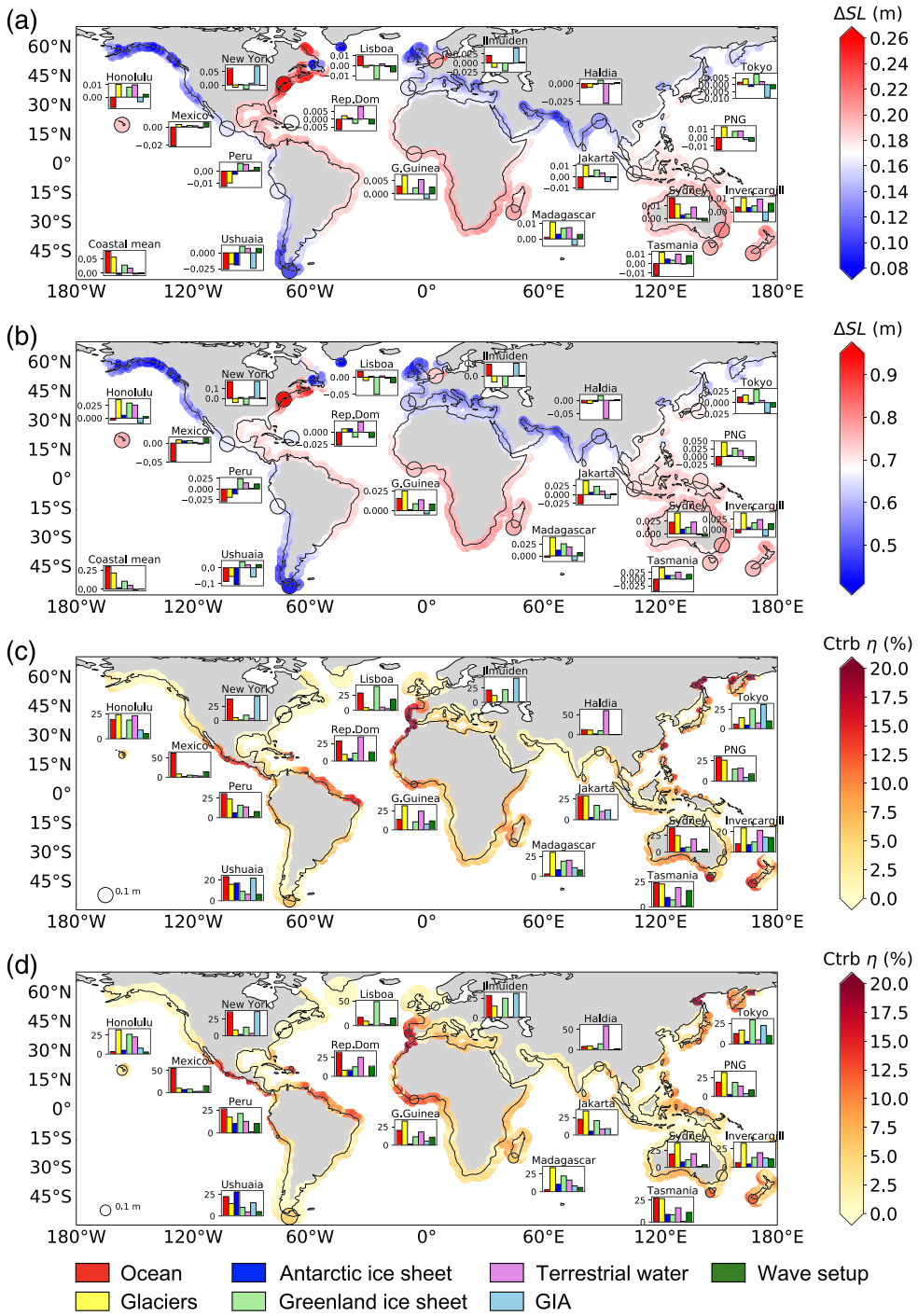

Figure 7. Spatial heterogeneity of the different contributions to projected coastal sea level changes. (a, b) Projected coastal SL changes (ΔSL) (sum of sterodynamic SL, glaciers, Antarctic ice sheet, Greenland ice sheet, terrestrial water, GIA, and wave setup computed with time-invariant beach slopes β_{gc}) from 1986–2005 to (a) 2026–2045 and (b) 2081–2100 under RCP8.5, shown as anomalies from the coastal global mean. The color bar is centered on the global coastal mean SL. The lower left inset shows the global coastal mean of each contributor to coastal SL changes. Other insets show regional anomalies of each contributor to the coastal SL changes from their own global coastal mean (see legend at the bottom), at different coastal grid points (indicated by black circles). Units are in meters. (c, d) Histograms showing the relative importance, in percentage, of each contributor (C_i) to the regional departure of coastal SL changes from the global mean coastal SL change. This is computed as, for contributor i:$|C_i'|/\Sigma|C_j'|.100$, where the prime denotes the local departure of the contributor i or j from its global coastal mean, and the sum is over j where j denotes the different contributions accounted for in this study. The colored dots along the coast show the contribution of the absolute value of regional anomalies of wave setup changes to the sum of absolute regional departure from GMSLR from each component (ctrb η), in percentage. The size of the colored dots indicates the amplitude of the absolute value of the departure from GMSLR (also given by the blue/red colormap in panels a and b), with a scaling on the lower left side of the panel. Panel c) is for 2026–2045, panel d) is for 2081–2100.

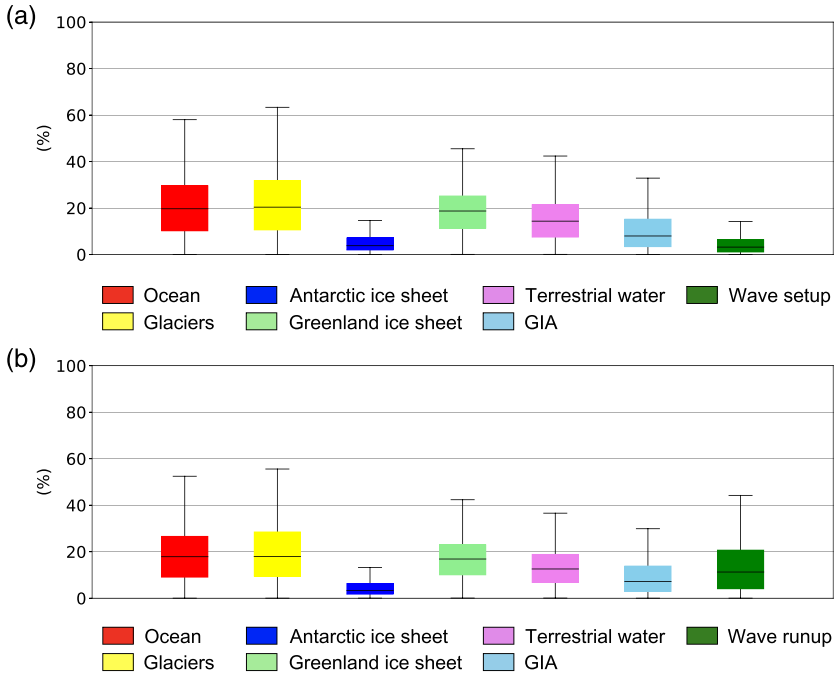

Figure 8. Contributions to regional departure from GMSLR. Boxplots of the relative contribution of each process (in %) to the regional departure of coastal SL changes from the GMSLR (averaged along the coast) for 2081–2100 relative to 1986–2005 under RCP8.5, considering (a) wave setup and (b) wave runup. Wave contributions were computed with a constant beach slopes of 0.04 (β_{gc}). Boxplots are computed from the distribution over all coastal points (60°N/60°S) of a given contributor to regional departure from GMSLR and represent the range Q1–1.5*IQR to Q3 + 1.5*IQR (black vertical line), the IQR (rectangle), and Q2 (median, horizontal line in the rectangle) where Q1, Q2, and Q3 are, respectively, the 1st, 2nd, and 3rd quartiles of the distribution and IQR the interquartile Q3–Q1.

with large population centers and locations with sizable projected wave setup changes (e.g., Figure 6). To illustrate the spatial heterogeneity of coastal SL components, their departure from averages along the world's coastlines (considering coasts equatorward of 60° in latitude, values are shown in lower left insets in Figures 7a and 7b) are chosen here rather than from global ocean mean values. The contribution of wave setup to coastal-GMSLR is close to zero (Figures 7a and 7b, lower left inset histograms) as expected. Indeed, wave setup changes analyzed here are only induced by changes in surface winds, and atmospheric circulation changes mostly average out at global scale. Coastal-GMSLR is dominated by the sterodynamic SL and glaciers mass loss. Over most of the world's coastlines, the sterodynamic contribution and glaciers mass loss also remain dominant contributors to projected spatial departure from coastal-GMSLR for the middle and end of the 21st century (Figures 7a and 7b).

The relative importance (in percentage) of each process to the spatial departure of coastal SL changes from coastal-GMSLR is shown in Figures 7c and 7d for the same coastal sites, while the specific contribution of wave setup is shown along the world coastlines. Wave setup changes appear as a substantial driver of local departure of coastal SL changes from GMSLR. As such, local wave setup changes can substantially compensate or add to local departure from global mean SL changes induced by other contributors (see also Figure 5 and section 3.2).

A more global view of the relative contribution of each process to the spatial departure from GMSLR along the world coastline is given in Figure 8a, and in Table 1 for the contribution of wave setup. The median of the contribution of wave setup to spatial departure from GMSLR over all coastal points is of 2–4%, and the 95th percentile reaches 9–14%. The contributions are similar when using β_{gc} or β_{gv} and are slightly larger for the middle than for the end of the 21st century and for the RCP8.5 scenario compared to the RCP4.5 scenario (Table 1). It should be noted that when using local estimates of the beach slope, or for other coastal environments, wave setup changes could be larger and explain a larger part of spatial departure from GMSLR (Figures 4 and 5 and section 4).

Table 1
First (Q1)/Second (Q2, in Bold)/Third (Q3) Quartile and Percentile 95 (P95, in Parenthesis) Values of Contribution Over All Coastal Sites (60°N/60°S) of Wave Setup to Regional Departure From GMSLR Referenced to the Historical Period, in Percentage

Q1/**Q2**/Q3 (P95) wave setup	Parameterization	Stockdon et al., 2006		Atkinson et al., 2017	
	Beach slope Scenario	β_{gc}	β_{gv}	β_{gc}	β_{gv}
MID21C	RCP4.5	1/**4**/7 (13)	2/**4**/7 (12)	1/**3**/7 (14)	1/**3**/7 (14)
MID21C	RCP8.5	1/**4**/7 (14)	2/**4**/7 (13)	2/**3**/7 (14)	2/**3**/7 (14)
END21C	RCP4.5	1/**2**/5 (9)	1/**2**/4 (9)	1/**2**/4 (9)	1/**2**/4 (9)
END21C	RCP8.5	1/**3**/6 (13)	1/**3**/6 (12)	1/**3**/6 (13)	1/**3**/6 (13)

4. Discussion

4.1. Projections of Runup

Swash corresponds to vertical fluctuations of the water line around the time mean wave setup and is one of the many processes causing changes in the shoreline position. The amplitude of these high-frequency oscillations can change with time, with a low-frequency modulation of the signal envelope. These changes in amplitude threaten the coast as they can generate coastal flooding through water overtopping or breaching of coastal defenses. Wave setup and swash add together making up the dynamical wave runup contribution (e.g., S06). The combination of all processes causing flooding (including setup and swash) provides relevant information for impact studies (e.g., Bouwer, 2018; Hinkel et al., 2015). For these reasons, we extend hereafter our analysis to discuss the projected changes in runup instead of setup over the 21st century.

Projected changes in wave runup induced by changes in (H_s, L_p) are of the same sign but of greater amplitude than changes in wave setup (equations 1 and 2) and exhibit similar patterns (Figure 9). Therefore, the relative importance of the wave runup contribution to spatial departure of coastal SL changes from GMSLR is larger (Figure 10) than when only wave setup is considered (Figure 7). As a result, runup contribution to regional departure from GMSLR can exceed 30% over extended portions of coastlines, such as along the tropical coasts of western America, the coasts of the African Bight, the coasts of southwestern Europe (Figure 10). It can be similar to the contribution of the sterodynamic SL or glaciers mass loss when using either a static beach slope of 0.04 (β_{gc}) or a dynamically adjusted and normalized beach slope (β_{gv}) (Figure 10). The median of the contribution of runup to spatial departure from GMSLR over all coastal points is in the range 8–14%, the third quantile in the range 14–23%, and the 95th percentile in the range 24–39% when using β_{gc} or β_{gv}, for changes at both the middle and end of the 21st century, and under RCP8.5 or RCP4.5 (Figure 8b and Table 2). As for wave setup, the contribution tends to be larger under RCP8.5 than under RCP4.5, for the middle than for the end of 21st century, and similar with β_{gc} or β_{gv}. The contribution of wave runup changes to spatial departure from GMSLR at the end of the 21st century can thus be substantial, with important consequences for coastal overtopping and flooding and the subsequent planning of risk protection and hazard mitigation.

4.2. Limitations of the Method to Estimate Wave Setup and Runup

Wave setup and runup can be predicted using different methodologies, such as direct numerical modeling with process-based local coastal models, metamodels, and empirical formulations (e.g., Dodet et al., 2019).

Process-based coastal models (such as, e.g., XBEACH, Roelvink et al., 2009) also need nearshore profiles as inputs, and cannot yet simulate wave setup and runup with nearshore morphological updating over long time scales and along the global coastline. In particular, the simulation of the beach profile evolution and morphological feedbacks at long time scales are hampered by limitations of the models in representing cross-shore sediment exchanges between the lower and upper part of the nearshore profile (e.g., Elsayed & Oumeraci, 2017).

Wave setup and runup are therefore commonly predicted via empirical formulations that relate them to a set of simple environmental parameters (see review by Dodet et al., 2019). As this study aims at providing a first-order global estimate of the contribution of wave setup and runup changes to coastal SL changes over long time scales (20-yr periods), wave setup and runup are computed using empirical formulae.

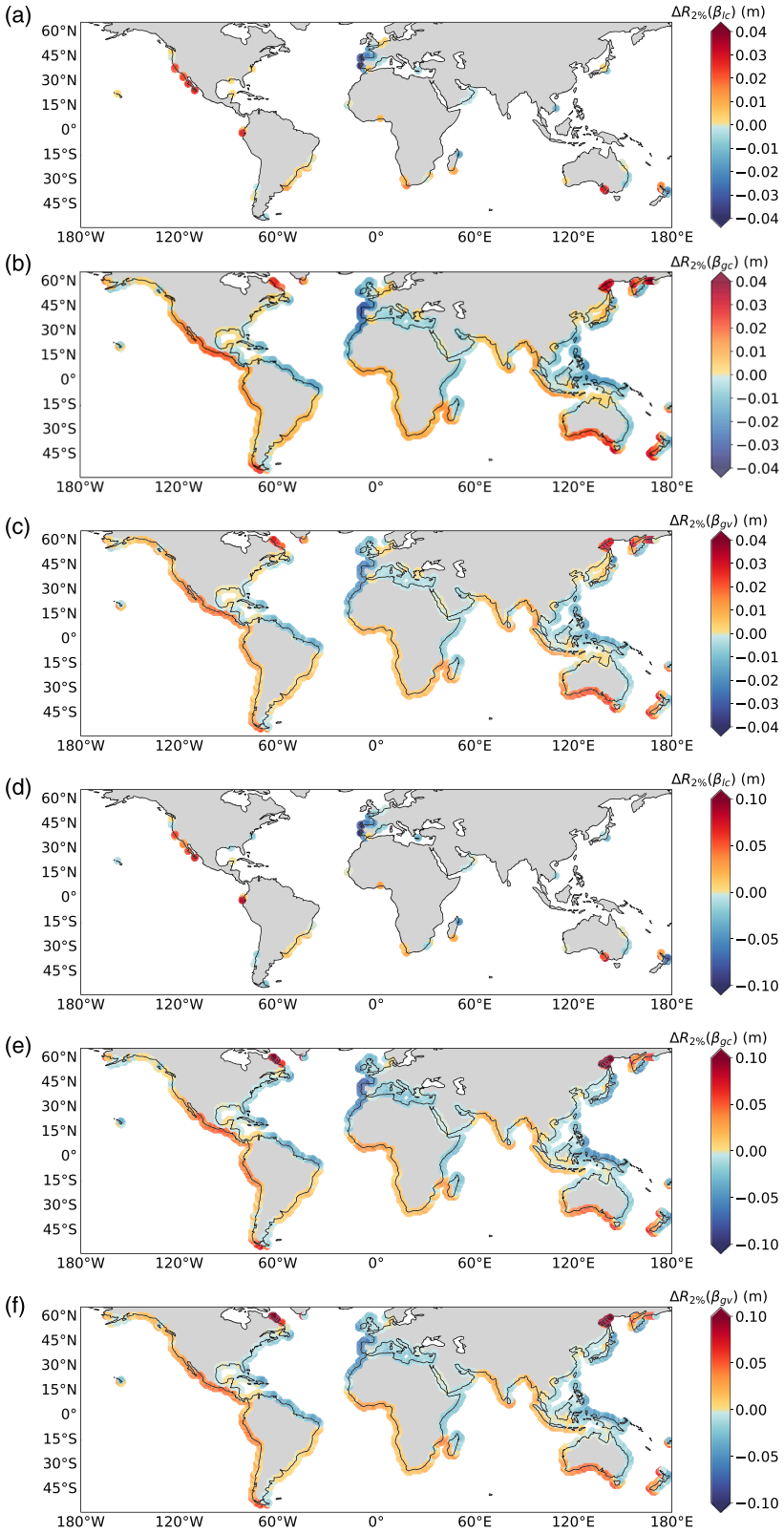

Figure 9. Projected runup changes. Projected ensemble mean runup changes from 1986–2005 to (a–c) 2026–2045 and (d–f) 2081–2100 under the RCP8.5 scenario, using (a, d) a local, time-invariant local beach slope (β_{lc}), (b, e), a time-invariant constant slope of 0.04 (β_{gc}), and (c, f) and a time-varying, normalized beach slope (β_{gv}). Units are in meters. Note the different color bars between panels (a)–(c) and (d)–(f).

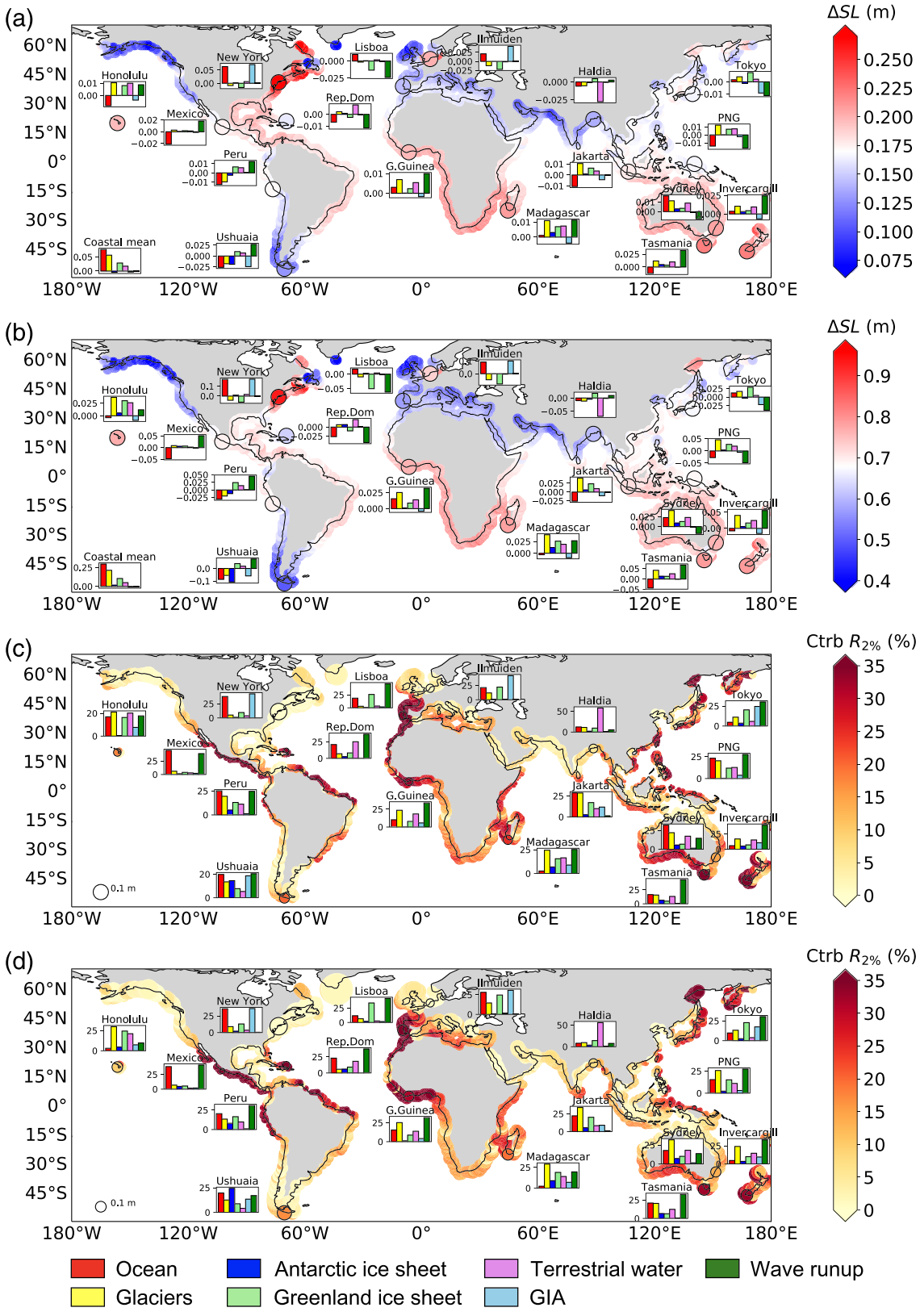

Figure 10. Spatial heterogeneity of the different contributions to projected coastal sea level changes, including runup. Same as Figure 7 but for wave runup changes instead of wave setup changes.

Table 2
First (Q1)/Second (Q2, in Bold)/Third (Q3) Quartile and Percentile 95 (P95, in Parenthesis) Contribution Over All Coastal Sites (60°N/60°S) of Wave Runup to Regional Departure From GMSLR Referenced to the Historical Period, in Percentage

Q1/**Q2**/Q3 (P95) wave runup	Parameterization	Stockdon et al. (2006)		Atkinson et al. (2017)	
		Beach slope			
	Scenario	β_{gc}	β_{gv}	β_{gc}	β_{gv}
MID21C	RCP4.5	5/**13**/23 (37)	6/**14**/22 (35)	4/**11**/21 (35)	5/**12**/19 (31)
MID21C	RCP8.5	5/**13**/23 (39)	6/**13**/23 (37)	4/**12**/21 (37)	5/**12**/20 (34)
END21C	RCP4.5	3/**9**/17 (27)	4/**9**/16 (27)	3/**8**/15 (26)	3/**8**/14 (24)
END21C	RCP8.5	4/**11**/21 (37)	5/**11**/20 (36)	3/**10**/19 (35)	4/**10**/18 (32)

Empirical formulation for wave setup and runup. A variety of empirical formulae exist to estimate wave setup and runup. Recent studies have extensively tested the most commonly used ones (e.g., Atkinson et al., 2017; Cohn & Ruggiero, 2016; Di Luccio et al., 2018; Díaz-Sánchez et al., 2014; Ji et al., 2018; O'Grady et al., 2019; Passarella et al., 2018; Power et al., 2019; Pullen et al., 2007; Sénéchal et al., 2011; Stockdon et al., 2014; Vousdoukas et al., 2012). These studies have shown the significant skills of these formulae in different study cases and their ability to outperform process-based models for $R_{2\%}$ (Stockdon et al., 2014). The scatter between empirically predicted and observed setup or runup can be due to second order processes (e.g., variability of the beach slope and nearshore morphological control on runup that is not captured when only accounting for the beach slope) that are not represented by the formulations' predictors (e.g., Díaz-Sánchez et al., 2014).

Wave setup and runup estimated from the S06 empirical formulations used here (equations 1 and 2) exhibit only relatively small differences from process-based models during modest wave conditions (Cohn & Ruggiero, 2016). Nonetheless, S06 formulations tend to underestimate runup (Atkinson et al., 2017; Power et al., 2019) especially during extremes (note that the formulations were calibrated under wave conditions that did not include extremes, Stockdon et al., 2014).

A sensitivity analysis of projected wave setup and runup changes to the choice of parameterizations used to estimate them is performed by computing wave setup and runup with the recent model-of-models formulation of Atkinson et al. (2017):

$$\eta = 0.16\, H_0 \tag{5}$$

$$R_{2\%} = 0.92\, tan\, \beta\, \sqrt{H_0 L_0} + 0.16 H_0 \tag{6}$$

The contribution of wave setup and runup to the spatial departure from GMSLR is found to be robust when using the Atkinson et al. (2017) formulations instead of the S06 formulations for both wave setup (Table 1) and runup (Table 2). This builds confidence in the reliability of the formulation used in our main analysis to estimate wave setup and runup.

Beach slope. The foreshore beach slope is an essential parameter in the estimation of wave setup and swash. Beach slopes generally range between 0.01 and 0.20 (Komar, 1998; Figure 1) and can substantially evolve over different time scales (events, seasonal, interannual, and in response to SLR, e.g., Aagaard & Hughes, 2017) and spatial scales (e.g., Madsen & Plant, 2001), from alongshore at a given local beach to regional scales (e.g., Díez et al., 2017; Karunarathna et al., 2016; Serafin et al., 2019). Cohn and Ruggiero (2016) studied the influence of nearshore morphological variability at seasonal to interannual time scales (sandbar position, changes in foreshore beach slope, and overall change in the bathymetric profile) on wave runup and found that natural variability in subaerial beach topography has a stronger influence than subtidal morphology change. Here, we partly account for morphological feedbacks by allowing beach face slope to evolve in response to changing incoming wave characteristics using the Sunamura (1984) formulation (equation 3). Limitations in the application of this formulation is that we kept the time mean of the beach slope unchanged (0.04), whereas it can be substantially different locally and lead to larger or smaller wave setup (Figure 4) or runup changes. We also used 6-hourly instantaneous wave characteristics to estimate the time-varying beach slope, whereas the adjustment times of the beach slope to changing wave

conditions is most likely longer, on the order of 1–10 days (Angnuureng et al., 2017; Madsen & Plant, 2001; Ranasinghe et al., 2012). Finally, the formulation was developed for hypothetical steady state conditions; it is not clear whether it can be used to predict the short-term temporal variation of the beach slope. In addition, local characteristics such as the beach or coast orientation can have substantial spatial variability. As our calculations are performed on a 1° × 1° grid, wave directions relative to the beach or coast orientation are not able to be resolved and are therefore not taken into account in our estimates. Therefore, waves are assumed to impinge perpendicularly on the coast and the influence of shelf bathymetry on wave conditions (shoaling, refraction) is not accounted for. Serafin et al. (2019) estimated a decrease of 5–10% of extreme runup events at three sites along the U.S. West Coast when accounting for wave transformation. Results such as these suggest that our estimates of the contribution of wave setup from waves impinging normally on the shoreline may be upper bound estimates. While change in offshore waves directions can be partly mitigated due to waves refraction processes, more local changes due to SL rise or bathymetric changes can also alter the local waves climate (e.g., Charles et al., 2012).

To extend calculations at global scale, we first chose a time and space constant beach slope value along the world's coastline. Such an approach is commonly used for regional to global-scale analysis (Vousdoukas et al., Vousdoukas, Mentaschi, Voukouvalas, Verlaan, et al., 2018; Serafin et al., 2017) since no observations of beach slopes applicable in parametric formulae (corresponding to the section of the beach where waves washup) is currently available worldwide (e.g., Luijendijk et al., 2018; Vousdoukas, Mentaschi, Voukouvalas, Bianchi, et al., 2018). We chose a beach slope value of 0.04, which represents the median value of the local values in the data set of 308 beach face slope used here. This median value is only an order of magnitude for natural beach slopes (Wright & Short, 1984; S06) and might be biased low due to the underrepresentation of tropical beaches in our data set. Wave setup change estimates can be scaled to the actual local slope of the beach as per equation 1 (see Figure 2c), provided that the local slope is within the range of applicability of the formula and assuming no changes in beach slope over the different period (see also discussion in the next subsection). As a result, the wave setup contribution may be twice as large as reported here for steep beach slopes, while on very gentle slopes, the contribution could be less than we present.

Applicability of the wave setup and runup empirical formulae to different coastal environments or beach slopes. The S06 formulae have been developed for natural sandy beaches over a wide range of dynamical conditions. Yet wave setup also exists in other type of environments (such as bays, fringing reefs, coastlines with marine vegetation, and rocky coasts) where the S06 wave setup formulation does not apply. Our calculations of wave setup and swash are performed on a 1° × 1° grid. At this resolution, coasts in a given coastal cell can include sandy beaches and other types of environments. Most coasts have a nonzero local percentage of sandy or gravel beaches over the world (Luijendijk et al., 2018, except notably in Indonesian seas and tropical western Pacific). In this paper, wave setup changes (and their contribution to total SLR) arise solely from changes in deep water wave characteristics. In our global estimates, these "regional climate wave setup changes" are only directly relevant for natural sandy beaches, which cover an estimated 31% of the world's ice-free coastlines (Luijendijk et al., 2018). Yet since several empirical formulations of wave setup and runup use a scaling in either (H_s) or in $(H_sL_p)^{0.5}$ (e.g., review by Dodet et al., 2019), as our estimate of wave setup changes does, our results of wave setup changes can be scaled to get indicative wave setup or runup changes computed with other beach slopes or empirical formulae. For runup on dikes, assuming an outer dike slope of 1/6 (representative for the German North Sea coast, Arns et al., 2017), leads to a runup that equals to $0.275(H_sL_p)^{0.5}$ using the Pullen et al. (2007) formulation, or $0.25(H_sL_p)^{0.5}$ using the Van der Meer and Stam (1992) formulation. Scaling our results for wave setup changes (Figures 2c and 3–5) by a factor or 19.6 or 17.9 therefore informs on wave runup changes over dikes with outer slopes of 1/6 using respectively Pullen et al. (2007) or Van der Meer and Stam (1992) formulations. For highly dissipative beaches, more specific formulations of setup and runup have been developed in S06. Using these dissipative-specific, beach slope-independent formulations compared to results reported here using the generic formulation with a globally constant foreshore beach slope of 0.04 would lead to similar results at first order (leading to an increase of wave setup by a factor 1.14 and decrease of runup by a factor 1.25).

Applicability of the wave setup empirical formula to long-term changes. In our analysis, 20-yr mean changes in wave setup and swash are calculated with empirical formulae that have been calibrated and/or validated with short observational time series of a few days to weeks, as is often the case for parameterizations in ocean sciences. We applied these formulae to 6-hourly wave outputs, but over long periods. This approach assumes

Table 3
(Top Rows) Antarctic Ice Sheet Contribution to GMSLR (Average Over the 60°N/60°S Coastal Sites) in Meters in Golledge et al., 2015 and Carson et al. (2016) (Note: SMB Is Negative and More so in RCP8.5 Than RCP4.5 in Carson et al. (2016) and the Dynamic Mass Loss Is Positive but Scenario Independent); (Bottom Rows) Median Value (in %) Over All Coastal Sites (60°N/60°S) of the Relative Contribution of the Antarctic Ice Sheet

	Antarctic ice sheet contribution to GMSLR (in m)			
	Carson et al., 2016		Golledge et al., 2015	
(m)	RCP4.5	RCP8.5	RCP4.5	RCP8.5
MID21C	−0.01	0.00	0.00	0.00
END21C	0.04	0.02	0.04	0.13
	Antarctic ice sheet contribution to regional departure from GMSLR (60°N/60°S coastlines) [wave setup with β_{gc}] (in %)			
	Carson et al., 2016		Golledge et al., 2015	
(%)	RCP4.5	RCP8.5	RCP4.5	RCP8.5
MID21C	2 [4]	2 [4]	>1 [4]	1 [4]
END21C	5 [2]	4 [3]	3 [3]	7 [3]

Note. The corresponding contribution of wave setup (using β_{gc}) to regional departure from GMSLR is indicated in bracket.

that the formulae are also valid for longer time scales than they have been calibrated for. Yet Power et al. (2019) noted that such formulae are prone to errors when applied outside the range of conditions (wave height, period, and beach slope) over which they have been calibrated. It could also be that morphodynamic feedbacks occur over longer time scales than the calibration period of the formulae. The relation between wave setup, runup, and beach morphodynamic response remains to be better understood.

It should be noted that the effects of systematic uncertainties on our estimates are potentially reduced by the fact that we focus on relative changes between different periods.

Interactions of wave setup with other contributors to SLR. Nonlinear interactions between components are unaccounted for in our estimates, although they can be substantial, for example, during storms (Idier et al., 2019). For instance, water depth changes induced by open ocean SL rise will lead to waves of greater amplitude and larger period breaking closer to the shore (Chini et al., 2010). This could result in higher runup and induce a need for amplified coastal protection design heights (Arns et al., 2017; Hoeke et al., 2015). SLR-induced change in wave conditions can exceed any atmospheric climate driven change in wave climate (Wandres et al., 2017). This effect is not included in the wave projections used in this analysis. Resolving interactions between the different contributors to coastal SL changes requires a fully coupled modeling approach (of tides, waves, ocean circulation, land ice, land hydrology) which is beyond current modeling capacities for the needed resolution.

4.3. Wave Model Resolution

The wave model simulations used in this paper come from a 1° resolution implementation of a spectral wave model. Many transformations of the wave field occur as they propagate across the shelf into shallower water (e.g., shoaling, refraction, and loss of energy from bottom friction), which will be poorly resolved in these coarse resolution simulations. These transformations will alter resultant changes in wave conditions at the breaking point (a key consideration for setup estimates) relative to those experienced offshore.

Together, these limitations (sections 4.2 and 4.3) may induce large uncertainties on our estimates in projected wave setup and runup changes. Our results therefore call for refined methodologies to estimate wave setup and runup at global scale and over a broad range of temporal scales.

4.4. Ice Sheets Contributions

Estimates of dynamical ice sheet mass loss are the main source of uncertainty for projected SL rise (e.g., de Winter et al., 2017; Kopp et al., 2017). The upper estimate used in our study (Katsman et al., 2011) does not include processes that could cause rapid and large mass loss of ice sheets such as the marine ice sheet instability (Ritz et al., 2015) and the marine ice cliff instability (DeConto & Pollard, 2016), the latter being associated with large uncertainties. We therefore complemented our results by using a more recent estimate of the Antarctic ice sheet contributions to SL rise, which considers the marine ice sheet instability (Golledge et al., 2015). We took the mean of the low and high estimates provided by Golledge et al. (2015) based on two different ice sheet parametrizations. The contribution of the Antarctic ice sheet to GMSLR is listed in Table 3. To regionalize this contribution, we used a fingerprint assuming that the contribution of Antarctica originates from west Antarctica, which is a shortcoming because East Antarctica could accumulate ice due to increased precipitations in a warmer climate. However, this approximation has minor effects far from the source, that is, in most coastal locations considered in this study. Using the Golledge et al. (2015) contribution for the Antarctic ice sheet instead of the one used in Carson et al. (2016) lead to similar contributions to GMSLR. It also leads to similar contributions of the Antarctic ice sheet and wave setup to regional departure from GMSLR (Table 3), except for the end of the 21st century under the RCP8.5 scenario. In that latter case, the Golledge et al. (2015) estimate is higher than the one used in Carson et al. (2016), leading to a

stronger contribution of the Antarctic ice sheet to regional departure from GMSLR along the coasts (7% instead of 4%, Table 3).

Regarding surface mass balance of the Greenland ice sheet, estimates in Slangen et al. (2014) used in our study are lower than (but in the same range as) estimates from regional climate models over Greenland forced by CMIP5 models, as in Fettweis et al. (2013).

Finally, other processes than considered here contribute to vertical land motions (including anthropogenic activities), which directly impact relative SL changes at the coast and can reach large values (e.g., Woodworth et al., 2019).

5. Conclusions

Wind waves are an important driver of coastal SL changes and are therefore of importance when considering the coastal hazards of flooding and erosion. As far as coastal SL is concerned, the focus on wind waves has thus far mostly been (i) on the contribution of wind waves to coastal SL, especially during extreme events, at local scales, and (ii) on past and projected changes in offshore wave climate (including interannual variability and trends). Bridging these two areas of research with projections of wind wave contributions to long-term coastal SL changes is the motivation of the present study. Based on empirical formulations, different estimates of beach slopes (locally reported values, globally constant, static, or time-evolving) and an ensemble of global wave models, we present a first-order estimate of the relative importance of the contribution of atmospheric climate driven wave setup changes to 20-yr mean projected coastal SL changes at global scale.

Projected 20-yr mean wave setup changes are overall small compared to dominant contributors to coastal SL changes (the ocean component and glacier mass loss), and even more so at the end of the century than at midcentury. Yet locally, 20-yr mean wave setup changes can be substantial compared to projected changes in other contributors of coastal SL change (the different land ice components and terrestrial water) over the 21st century. The amplitude of wave setup changes depends on the value of the beach slope used.

When averaged over the world coastlines, wave setup changes mostly average out as wave setup changes considered here solely arise from changes in surface winds. They are therefore much more limited than SL rise due to land ice mass loss or the thermal expansion of the ocean. The latter is expected to continue for centuries as it is only limited by the amount of heat excess in the climate system that can be stored in the ocean.

Regional patterns of projected wave setup changes are heterogeneous but consistent over large portions of the world coastline. The spatial variability and amplitude of wave setup changes make wave setup a small yet substantial contributor to spatial departures of coastal SL changes from global mean (along the coastlines between 60°N/60°S) SL rise (GMSLR), with a median contribution along the coastlines of about 2–4%, and the 95th percentile reaching 9–14% across the different scenarios for beach slopes and 21st century 20-yr periods. However, the wave setup contribution could be larger locally, especially for beaches with slopes greater than the global constant of 0.04 used here. Thus, wave setup changes can substantially either enhance or reduce local coastal SL changes departure from GMSLR due to other contributors such as sterodynamic effects and should be included in regional patterns of coastal SL changes.

When considering wave runup 20-yr mean changes, incorporating changes in swash amplitude in addition to wave setup changes, wave contributions to local departure from GMSLR are larger with a median contribution along the coastlines of about 8% to 14% across the different scenarios for beach slopes and 21st century 20-yr periods and a 95th percentile reaching 24–39%.

Changes in other components of SL will further influence the wave setup contribution, which we are unable to resolve here at global scale, for example, via depth modulation of the wave field associated with SLR (Arns et al., 2017; Hoeke et al., 2015; Idier et al., 2019). As the frequency of marine flooding events is expected to grow dramatically over the coming decades due to a committed SL rise of a few tens of centimeters (e.g., Oppenheimer et al., 2019; Vitousek et al., 2017), our results indicate that accounting for nonstationary wave contributions to projected low-frequency coastal SL changes can modify extreme events frequency and severity. It should be noted though that projections of the changes in mean wave conditions do not necessarily represent projected changes in wave extremes (Morim et al., 2018). Changes in frequency or intensity of

extreme wave events may lead to wave setup changes at high frequency different from the ones presented here, and offer greater contributions to coastal SL. As more physical processes are being included in global coastal impact models (Bouwer, 2018; Hallegatte et al., 2013; Hinkel et al., 2014), our results advocate for the inclusion of nonstationary wave contributions to projected coastal SL changes in these models to provide more accurate assessments and better inform policy decisions. Wave contributions to coastal SL changes are also sensitive to changes in wave direction, disregarded here. Roughly 20% of the world's coasts are exposed to risk associated with robust projected changes in wave direction.

Quantifying adaptation needs at global scale is a research challenge (e.g., Bouwer, 2018), especially at time scales relevant for decision making such as the coming decades. As different processes contributing to coastal SL changes as well as changes at different time scales (from extreme events to long-term SLR) have different adverse effects on the coasts (coastline erosion and shoreline retreat, flooding, saltwater intrusion in aquifers and surface water, and potential decline of coastal wetlands such as mangroves and salt marshes), there is a need to better understand the drivers of low-frequency changes in projected coastal SL changes, including at long time scales. This study contributes to that goal by suggesting a substantial contribution of wave setup changes to 20-yr mean local departure of coastal SL from GMSLR over a large portion of the world's coastline during the 21st century even though wave setup changes are currently nonaccounted for in global-scale coastal SL projections and risk assessment.

Conflict of Interest

The authors declare no any real or perceived financial conflicts of interests.

Data Availability Statement

Data availability is detailed in section 2. Contributions to relative sea level changes accounted for in IPCC AR5 projections are available at the Integrated Climate Data Center (ICDC, https://icdc.cen.uni-hamburg.de/1/daten/ocean/coastal-sea-level-changes.html). Wave climate projections are available at CSIRO (http://data-cbr.csiro.au/thredds/catalog/catch_all/CMAR_CAWCR-Wave_archive/Global_wave_projections/catalog.html). Analyses and figures were done with Python.

Acknowledgments

The authors thank two anonymous reviewers as well as Mark Carson for helpful comments leading to improvements in the manuscript. M. H. is supported by the Australian Government National Environmental Science Program Earth Systems and Climate Change Hub. G. L. C. is supported by the ERA4CS ECLISEA project (Grant 690462). R. A. is supported by a French ANR grant (COASTVAR ANR-14-ASTR-0019). The authors are grateful to Dr. Omar Defeo for providing us with their data set of beach slopes and sediment grain sizes.

References

Aagaard, T., & Hughes, M. G. (2017). Equilibrium shoreface profiles: A sediment transport approach. *Marine Geology*, *390*, 321–330. https://doi.org/10.1016/j.margeo.2016.12.013

Almar, R., Blenkinsopp, C., Almeida, L. P., Bergsma, E. W. J., Catalan, P. A., Cienfuegos, R., & Viet, N. T. (2019). Intertidal beach profile estimation from reflected wave measurements. *Coastal Engineering*, *151*, 58–63. https://doi.org/10.1016/j.coastaleng.2019.05.001

Angnuureng, D., Almar, R., Sénéchal, N., Castelle, B., Appeaning Addo, K., & Marieu, V. (2017). Shoreline evolution under sequences of storms from video observations at a meso-macrotidal barred beach. *Geomorphology*, *290*, 265–276. https://doi.org/10.1016/j.geomorph.2017.04.007

Arns, A., Dangendorf, S., Jensen, J., Talke, S., Bender, J., & Pattiaratchi, C. (2017). Sea-level rise induced amplification of coastal protection design heights. *Scientific Reports*, *7*(1), 40,171. https://doi.org/10.1038/srep40171

Atkinson, A. L., Power, H. E., Moura, T., Hammond, T., Callaghan, D. P., & Baldock, T. E. (2017). Assessment of runup predictions by empirical models on non-truncated beaches on the south-east Australian coast. *Coastal Engineering*, *119*, 15–31. https://doi.org/10.1016/j.coastaleng.2016.10.001

Barboza, R., & Defeo, O. (2015). Global diversity patterns in sandy beach macrofauna: A biogeographic analysis. *Scientific Reports*, *5*(1), 14,515. https://doi.org/10.1038/srep14515

Bascom, W. N. (1951). The relationship between sand size and beach-face slope, transactions. *American Geophysical Union*, *32*(6), 866–874. https://doi.org/10.1029/TR032i006p00866

Bouwer, L. M. (2018). Next-generation coastal risk models. *Nature Climate Change*, *8*(9), 765–766. https://doi.org/10.1038/s41558-018-0262-2

Bujalesky, G. G. (2007). Coastal geomorphology and evolution of Tierra del Fuego (Southern Argentina), *Geologica Acta*, Vol.*5*(4), 337–362

Carranza-Edwards, A., Bocanegra-Garcia, G., Rosales-Hoz, L., & de Pablo Galàn, L. (1998). Beach sands from Baja California Peninsula. *Mexico, Sedimentary Geology*, *119*(3-4), 263–274. https://doi.org/10.1016/S0037-0738(98)00066-9

Carrasco, A. R., O. Ferreira, P. Freire, J.A. Dias (2009). Morphological changes in a low-energy backbarrier. *Journal of Coastal Research*, SI 56 (Proceedings of the 10th International Coastal Symposium), 173–177.

Carson, M., Kohl, A., Stammer, D., Slangen, A. B. A., Katsman, C. A., van de Wal, R. S. W., et al. (2016). Coastal sea level changes, observed and projected during the 20th and 21st century. *Climatic Change*, *134*(1-2), 269–281. https://doi.org/10.1007/s10584-015-1520-1

Cazenave, A., & Le Cozannet, G. (2014). Sea level rise and its coastal impacts. *Earth's Future*, *2*(2), 15–34. https://doi.org/10.1002/2013EF000188

Cesaraccio, M., Thomas, Y. F., Diaw, A. T., & Ouegnimaoua, L. (2004). Impact of sand extractions on coastal dynamics Sarène Point beach. *Senegal, Géomorphologie: relief, processus, environement*, *1*, 55–64.

Charles, E., Idier, D., Delecluse, P., Déqué, M., & Le Cozannet, G. (2012). Climate change impact on waves in the Bay of Biscay, France. *Ocean Dynamics*, *62*(6), 831–848. https://doi.org/10.1007/s10236-012-0534-8

Chini, N., Stansby, P., Leake, J., Wolf, J., Roberts-Jones, J., & Lowe, J. (2010). The impact of sea level rise and climate change on inshore wave climate: A case study for East Anglia (UK). *Coastal Engineering*, *57*(11-12), 973–984. https://doi.org/10.1016/j.coastaleng.2010.05.009

Church, J. A., Clark, P. U., Cazenave, A., Gregory, J. M., Jevrejeva, S., Levermann, A., et al. (2013). Sea level change. In T. F. Stocker, D. Qin, G.-K. Plattner, M. Tignor, S. K. Allen, J. Boschung, A. Nauels, Y. Xia, V. Bex, & P. M. Midgley (Eds.), *Climate change 2013: The physical science basis. Contribution of Working Group I to the Fifth Assessment Report of the Intergovernmental Panel on Climate Change* (pp. 1137–1216). Cambridge, UK and New York, NY: Cambridge University Press.

Cohn, N., & Ruggiero, P. (2016). The influence of seasonal to interannual nearshore profile variability on extreme water levels: Modeling wave runup on dissipative beaches. *Coastal Engineering*, *115*, 79–92. https://doi.org/10.1016/j.coastaleng.2016.01.006

Cuevas, E., de los Angeles Liceaga-Correa, M., & Mariño-Tapia, I. (2010). Influence of beach slope and width on hawksbill (Eretmochelys imbricata) and Green Turtle (Chelonia mydas) nesting activity in El Cuyo, Yucatán, Mexico. *Chelonian Conservation and Biology*, *9*(2), 262–267. https://doi.org/10.2744/CCB-0819.1

de Winter, R. C., Reerink, T. J., Slangen, A. B. A., de Vries, H., Edwards, T., & van de Wal, R. S. W. (2017). Impact of asymmetric uncertainties in ice sheet dynamics on regional sea level projections. *Natural Hazards and Earth System Sciences*, *17*(12), 2125–2141. https://doi.org/10.5194/nhess-17-2125-2017

DeConto, R. M., & Pollard, D. (2016). Contribution of Antarctica to past and future sea-level rise. *Nature*, *531*(7596), 591–597. https://doi.org/10.1038/nature17145

Di Luccio, D., Benassai, G., Budillon, G., Mucerino, L., Montella, R., & Pugliese Carratelli, E. (2018). Wave run- up prediction and observation in a micro-tidal beach. *Natural Hazards and Earth System Sciences Discussion*, *18*(11), 2841–2857. https://doi.org/10.5194/nhess-18-2841-2018

Díaz-Sánchez, R., López-Gutiérrez, J. S., Lechuga, A., & Negro, V. (2014). Runup variability due to time dependence and stochasticity in the beach profiles: Two extreme cases of the Spanish coast. *Journal of Coastal Research*, *70*(sp1), 1–6. https://doi.org/10.2112/SI70-001.1

Díez, J., Uriarte, A., Cánovas, V., & Medina, R. (2017). A parametric model for dry beach equilibrium profiles. *Coastal Engineering*, *127*, 134–144. https://doi.org/10.1016/j.coastaleng.2017.06.012

Dodet, G., Melet, A., Ardhuin, F., Almar, R., Bertin, X., Idier, D., & Pedreros, R. (2019). The contribution of wind generated waves to coastal sea level changes. *Surveys in Geophysics*, *40*(6), 1563–1601. https://doi.org/10.1007/s10712-019-09557-5

Elsayed, S. M., & Oumeraci, H. (2017). Effect of beach slope and grain-stabilization on coastal sediment transport: An attempt to overcome the erosion overestimation by XBeach. *Coastal Engineering*, *121*, 179–196. https://doi.org/10.1016/j.coastaleng.2016.12.009

Familkhalili, R., & Talke, S. A. (2016). The effect of channel deepening on storm surge: Case study of Wilmington, NC. *Geophysical Research Letters*, *43*(17), 9138–9147. https://doi.org/10.1002/2016GL069494

Fan, Y., Lin, S.-J., Griffies, S. M., & Hemer, M. A. (2014). Simulated global swell and wind-sea climate and their responses to anthropogenic climate change at the end of the twenty-first century. *Journal of Climate*, *27*(10), 3516–3536. https://doi.org/10.1175/JCLI-D-13-00198.1

Fettweis, X., Franco, B., Tedesco, M., van Angelen, J. H., Lenaerts, J. T. M., van den Broeke, M. R., & Gallee, H. (2013). Estimating the Greenland ice sheet surface mass balance contribution to future sea level rise using the regional atmospheric climate model MAR. *The Cryosphere*, *7*(2), 469–489. https://doi.org/10.5194/tc-7-469-2013

Forget, G., & Ponte, R. M. (2015). The partition of regional sea level variability. *Progress. Oceanogr.*, *137*, 173–195. https://doi.org/10.1016/j.pocean.2015.06.002

Gainza, J., Rueda, A., Camus, P., Tomás, A., Méndez, F. J., Sano, M., & Tomlinson, R. (2018). A meta-modelling approach for estimating long-term wave run-up and total water level on beaches. *Journal of Coastal Research*, *34*, 475–489.

Golledge, N. R., Kowalewski, D. E., Naish, T. R., Levy, R. H., Fogwill, C. J., & Gasson, E. G. W. (2015). The multi-millennial Antarctic commitment to future sea-level rise. *Nature*, *526*(7573), 421–425. https://doi.org/10.1038/nature15706

Gregory, J. M., Griffies, S. M., Hughes, C. W., Lowe, J. A., Church, J. A., Fukimori, I., et al. (2019). Concepts and terminology for sea level-mean, variability and change, both local and global. *Surveys in Geophysics*, *40*(6), 1251–1289. https://doi.org/10.1007/s10712-019-09525-z

Hallegatte, S., Green, C., Nicholls, R. J., & Corfee-Morlot, J. (2013). Future flood losses in major coastal cities. *Nature Climate Change*, *3*(9), 8026.

Harley, M. D. I., Turner, L., Kinsela, M. A., Middleton, J. H., Mumford, P. J., Splinter, K. D., et al. (2017). Extreme coastal erosion enhanced by anomalous extratropical storm wave direction. *Scientific Reports*, *7*(1), 6033. https://doi.org/10.1038/s41598-017-05792-1

Hemer, M. A., Fan, Y., Mori, N., Semedo, A., & Wang, X. L. (2013). Projected future changes in wind-wave climate in a multi-model ensemble. *Nature Climate Change*, *3*(5), 471–476. https://doi.org/10.1038/nclimate1791

Hemer, M. A., & Trenham, C. E. (2016). Evaluation of a CMIP5 derived dynamical global wind wave climate model ensemble. *Ocean Modelling*, *103*, 190–203. https://doi.org/10.1016/j.ocemod.2015.10.009

Hinkel, J., Jaeger, C., Nicholls, R. J., Lowe, J. A., Renn, O., & Peijun, S. (2015). Sea-level rise scenarios and coastal risk management. *Nature Climate Change*, *5*(3), 188–190. https://doi.org/10.1038/nclimate2505

Hinkel, J., Lincke, D., Vafeidis, A. T., Perrette, M., Nicholls, R. J., Tol, R. S., et al. (2014). Coastal flood damage and adaptation costs under 21st century sea-level rise. *Proceedings of the National Academy of Sciences*, *111*(9), 3292–3297. https://doi.org/10.1073/pnas.1222469111

Hoeke, R. K., McInnes, K. L., Kruger, J. C., McNaught, R. J., Hunter, J. R., & Smithers, S. G. (2013). Widespread inundation of Pacific islands triggered by distant-source wind-waves. *Global and Planetary Change*, *108*, 128–138. https://doi.org/10.1016/j.gloplacha.2013.06.006

Hoeke, R. K., McInnes, K. L., & O'Grady, J. G. (2015). Wind and wave setup contributions to extreme sea levels at a tropical High Island: A stochastic cyclone simulation study for Apia, Samoa. *J. Mar. Sci. Eng.*, *3*(3), 1117–1135. https://doi.org/10.3390/jmse3031117

Hongo, C., Kurihara, H., & Golbuu, Y. (2018). Projecting of wave height and water level on reef-lined coasts due to intensified tropical cyclones and sea level rise in Palau to 2100. *Natural Hazards and Earth System Sciences*, *18*(2), 669–686. https://doi.org/10.5194/nhess-18-669-2018

Idier, D., Bertin, X., Thompson, P., & Pickering, M. D. (2019). Interactions between mean sea-level, tide, surge and flooding: Mechanisms and contributions to sea level variations at the coast. *Surveys in Geophysics*, *40*, 1603–1630.

Isla, F. I., & Bujalesky, G. G. (2005). Groundwater dynamics on macrotidal gravel beaches of Tierra del Fuego, Argentina. *J. of Coastal Research*, *211*, 65–72. https://doi.org/10.2112/02102.1

Ivamy, M. C., & Kench, P. S. (2006). Hydrodynamics and morphological adjustment of a mixed sand and gravel beach. *Torere, Bay of Plenty, New Zealand, Marine Geology*, *228*, 137–152.

Ji, C., Zhang, Q., & Wu, Y. (2018). An empirical formula for maximum wave setup based on a coupled wave-current model. *Ocean Engineering*, *147*, 215–226. https://doi.org/10.1016/j.oceaneng.2017.10.021

Karunarathna, H., Caraballo, J.-H., Kuriyama, Y., Mase, H., Ranasinghe, R., & Reeve, D. E. (2016). Linkages between sediment composition, wave climate and beach profile variability at multiple timescales. *Marine Geology*, *381*, 194–208. https://doi.org/10.1016/j.margeo.2016.09.012

Katsman, C. A., and Coauthors (2011). Exploring high-end scenarios for local sea level rise to develop flood protection strategies for a low-lying delta—The Netherlands as an example, *Climatic Change*, *109*(3-4), 617, 645. https://doi.org/10.1007/s10584-011-0037-5

Komar, P. (1998). Beach processes and sedimentation. 2nd ed. (prentice hall, upper Saddle River, 1998).

Kopp, R. E., DeConto, R. M., Bader, D. A., Hay, C. C., Horton, R. M., Kulp, S., et al. (2017). Evolving understanding of Antarctic ice-sheet physics and ambiguity in Probabilistic Sea-level projections. *Earth's Future*, *5*(12), 1217–1233. https://doi.org/10.1002/2017EF000663

Kuriyama, Y., Banno, M., & Suzuki, T. (2012). Linkages among interannual variations of shoreline, wave and climate at Hasaki. *Japon, Geophysical Research Letters*, *39*, L06604.

Lefebvre, J.-P., Almar, R., Viet, N. T., Uu, D. V., Thuan, D. H., Binh, L. T., et al. (2014). Contribution of swash processes generated by low energy wind waves in the recovery of a beach impacted by extreme even Trang, Vietnam. *Journal of Coastal Research*, *sp70*, 6.

Lentz, E. E., Thieler, E. R., Plant, N. G., Stippa, S. R., Horton, R. M., & Gesch, D. B. (2016). Evaluation of dynamic coastal response to sea-level rise modifies inundation likelihood. *Nature Climate Change*, *6*(7), 696–700. https://doi.org/10.1038/nclimate2957

Luijendijk, A., Hagenaars, G., Ranasinghe, R., Baart, F., Donchyts, G., & Aarninkhof, S. (2018). The state of the world's beaches. *Scientific Reports*, *8*(1), 6641. https://doi.org/10.1038/s41598-018-24630-6

Madsen, A. J., & Plant, N. G. (2001). Intertidal beach slope predictions compared to field data. *Marine Geology*, *173*(1-4), 121–139. https://doi.org/10.1016/S0025-3227(00)00168-7

Maurer, A. S., & Johnson, M. W. (2017). Loggerhead nesting in the northern Gulf of Mexico: Importance of beach slope to nest site selection in the Mississippi Barrier Islands. *Chelonian Conservation and Biology*, *16*(2), 250–254. https://doi.org/10.2744/CCB-1256.1

Meehl, G. A., Stocker, T. F., Collins, W. D., Friedlingstein, P., Gaye, A., Gregory, J., et al. (2007). Global climate projections. In S. Solomon, D. Qin, M. Manning, Z. Chen, M. Marquis, K. B. Averyt, M. Tignor, & H. L. Miller (Eds.), *Climate change 2007: The physical science basis. Contribution of Working Group 1 to the Fourth Assessment Report of the Intergovernmental Panel on Climate Change* (pp. 747–846). Cambridge: Cambridge University Press. https://www.ipcc.ch/site/assets/uploads/2018/02/ar4-wg1-chapter10-1.pdf

Melet, A., Almar, R., & Meyssignac, B. (2016). What dominates sea level at the coast: A case study for the Gulf of Guinea. *Ocean Dynamics*, *66*(5), 623–636. https://doi.org/10.1007/s10236-016-0942-2

Melet, A., Meyssignac, B., Almar, R., & Le Cozannet, G. (2018). Under-estimated wave contribution to sea-level rise. *Nature Climate Change*, *8*(3), 234–239. https://doi.org/10.1038/s41558-018-0088-y

Mentaschi, L., Vousdoukas, M. I., Voukouvalas, E., Dosio, A., & Feyen, L. (2017). Global changes of extreme coastal wave energy fluxes triggered by intensified teleconnection patterns. *Geophysical Research Letters*, *44*, 2416–2426. https://doi.org/10.1002/2016GL072488

Meyssignac, B., Slangen, A. B. A., Melet, A., Church, J., Fettweis, X., Marzeion, B., et al. (2017). Evaluating model simulations of twentieth-century sea-level rise. *Part II: Regional sea-level change, Journal of Climate*, *30*, 8565–8593.

Mori, N., Shimura, T., Yoshida, K., Mizuta, R., Okada, Y., Fujita, M., et al. (2019). Future changes in extreme storm surges based on mega-ensemble projection using 60-km resolution atmospheric global circulation model. *Coastal Engineering Journal*, *61*(3), 295–307. https://doi.org/10.1080/21664250.2019.1586290

Morim, J., Hemer, M. A., Cartwright, N., Strauss, D., & Andutta, F. (2018). On the concordance of 21st century wind-wave climate projections. *Global and Planetary Change*, *167*, 160–171. https://doi.org/10.1016/j.gloplacha.2018.05.005

Morim, J., Hemer, M. A., et al. (2019). Robustness and uncertainties in global multivariate wind-wave climate projections. *Nature Climate Change*, *9*(9), 711–718. https://doi.org/10.1038/s41558-019-0542-5

Moss, R. H., Edmonds, J. A., Hibbard, K. A., Manning, M. R., Rose, S. K., Van Vuuren, D. P., et al. (2010). The next generation of scenarios for climate change research and assessment. *Nature*, *463*(7282), 747–756. https://doi.org/10.1038/nature08823

Neumann, B., Vafeidis, A. T., Zimmermann, J., & Nicholls, R. J. (2015). Future coastal population growth and exposure to sea-level rise and coastal flooding—A global assessment. *PLoS ONE*, *10*(3), e0118571. https://doi.org/10.1371/journal.pone.0118571

Norcross, Z. M., Fletcher, C. H., & Merrifield, M. (2002). Annual and interannual changes on a reef-fringed pocket beach: Kailua Bay. *Hawaii, Marine Geology*, *190*(3-4), 553–580. https://doi.org/10.1016/S0025-3227(02)00481-4

O'Grady, J., McInnes, K. L., Hemer, M. A., Hoeke, R., Stephenson, A., & Colberg, F. (2019). Extreme water levels for Australian beaches using empirical equations for shoreline wave setup. *Journal of Geophysical Research: Oceans*, *124*, 5468–5484.

Oppenheimer, M., Glavovic, B. C., Hinkel, J., van de Wal, R., Magnan, A. K., Abd-Elgawad, A., et al. (2019). Sea level rise and implications for low lying islands, coasts and communities. In H.-O. Pörtner, et al. (Eds.), *IPCC Special Report on the Ocean and Cryosphere in a Changing Climate* (169 pp.). https://report.ipcc.ch/srocc/pdf/SROCC_FinalDraft_Chapter4.pdf

Passarella, M., De Muro, S., Ruju, A., & Coco, G. (2018). An assessment of swash excursion predictors using field observations. *Journal of Coastal Research*, *85*, 1036–1040. https://doi.org/10.2112/SI85-208.1

Pedreros, R., D. Idier, H. Muller, S. Lecacheux, F. Paris, M. Yates-Michelin, et al. (2018). Relative contribution of wave setup to the storm surge: observations and modeling based analysis in open and protected environments (Truc Vert beach and Tubuai island). In: Shim, J.-S. (eds.), Proceedings from the International Coastal Symposium (ICS) 2018 (Busan, Republic of Korea). *Journal of Coastal Research*, *85*, 1046–1050. Coconut Creek (Florida), ISSN 0749–0208.

Peltier, W. R. (2004). Global glacial isostasy and the surface of the ice-age Earth: The ice-5G (VM2) model and grace. *Annual Review of Earth and Planetary Sciences*, *32*(1), 111–149. https://doi.org/10.1146/annurev.earth.32.082503.144359

Peltier, W. R., Argus, D. F., & Drummond, R. (2015). Space geodesy constrains ICE age terminal deglaciation: The global ICE-6G_C (VM5a) model. *Journal of Geophysical Research: Solid Earth*, *120*, 450–487. https://doi.org/10.1002/2014JB011176

Pino, M., & Jaramillo, E. (1992). Morphology, texture and mineralogical composition of sandy beaches in the south of Chile. *Journal of Coastal Research*, *8*(3), 593–602.

Ponte, R. M., Carson, M., Cirano, M., Domingues, C. M., Jevrejeva, S., Marcos, M., et al. (2019). Towards comprehensive observing and modeling systems for monitoring and predicting regional to coastal sea level. *Frontiers in Marine Science*, *6*, 437. https://doi.org/10.3389/fmars.2019.00437

Poulos, S. E., Plomaritis, T. A., Ghionis, G., Collins, M. B., & Angelopoulos, C. (2013). The role of coast influencing sea level variations induced by meteorological forcing in microtidal waters: Examples from the island of Crete (Aegean Sea, Greece). *Journal of Coastal Research*, *29*(2), 272–282.

Power, H. E., Gharabaghi, B., Bonakdari, H., Robertson, B., Atkinson, A. L., & Baldock, T. E. (2019). Prediction of wave runup on beaches using Gene-Expression Programming and empirical relationships. *Coastal Engineering*, *144*, 47–61. https://doi.org/10.1016/j.coastaleng.2018.10.006

Pullen, T., Allsop, N. W. H., Bruce, T., Kortenhaus, A., Schüttrumpf, H., Van der Meer, J. W., et al. & EurOtop (2007). Wave overtopping of sea defences and related structures: Assessment manual. Heide, Holst.: Boyens (Die Küste; 73). - ISBN 978–3–8042-1064-6.
Quilfen, Y., Yurovskaya, M., Chapron, B., & Ardhuin, F. (2018). Storm waves focusing and steepening in the Agulhas current: Satellite T observations and modeling. *Remote Sensing of Environment*, *216*, 561–571. https://doi.org/10.1016/j.rse.2018.07.020
Ranasinghe, R., Holman, R., de Schipper, M., Lippmann, T., Wehof, J., Minh Duong, T., et al. (2012). Quantifying nearshore morphological recovery time scales using argus video imaging: Palm Beach, Sydney and Duck, North Carolina. *Coastal Engineering Proceedings*, *1*(33), 24. https://doi.org/10.9753/icce.v33.sediment.24
Reguero, B. G., Losada, I. J., & Méndez, F. J. (2019). A recent increase in global wave power as a consequence of oceanic warming. *Nature Communications*, *10*(1), 205. https://doi.org/10.1038/s41467-018-08066-0
Reis, A. H., & Gama, C. (2009). Sand size versus beachface slope—An explanation based on the constructal law. *Geomorphology*, *114*, 276–283.
Ritz, C., Edwards, T. L., Durand, G., Payne, A. J., Peyaud, V., & Hindmarsh, R. C. (2015). Potential sea-level rise from Antarctic ice-sheet instability constrained by observations. *Nature*, *528*(7580), 115–118. https://doi.org/10.1038/nature16147
Rodríguez-Polo, S., Del Río, L., & Benavente, J. (2018). Longitudinal distribution of slope and sediment characteristics in headland-bay beaches in Cádiz, Spain. *Journal of Coastal Research*, *85*(sp1), 306–310.
Roelvink, D., Reniers, A., van Dongeren, A., van Thiel de Vries, J., McGall, R., & Lescinski, J. (2009). Modelling storm impacts on beaches, dunes and barrier islands. *Coastal Engineering*, *56*(11-12), 1133–1152. https://doi.org/10.1016/j.coastaleng.2009.08.006
Rueda, A., Vitousek, S., Camus, P., Tomas, A., Epejo, A., Losada, I. J., et al. (2017). Global classification of coastal flooding climates. *Scientific Reports*, *7*(1), 5038. https://doi.org/10.1038/s41598-017-05090-w
Ruggiero, P. (2013). Is the intensifying wave climate of the U.S. Pacific Northwest increasing flooding and erosion risk faster than sea level rise? *Journal of Waterway, Port, Coastal, and Ocean Engineering*, *139*(2), 88–97. https://doi.org/10.1061/(ASCE)WW.1943-5460.0000172
Semedo, A., Suselj, K., Rutgersson, A., & Sterl, A. (2011). A global view on the wind sea and swell climate and variability from ERA-40. *Journal of Climate*, *24*(5), 1461–1479. https://doi.org/10.1175/2010JCLI3718.1
Sénéchal, N. (2017). Alongshore variability in observed runup under dissipative conditions. *Coastal Dynamics*, *208*.
Sénéchal, N., Coco, G., Bryan, K. R., & Holman, R. A. (2011). Wave runup during extreme storm conditions. *Journal of Geophysical Research*, *116*, C07032. https://doi.org/10.1029/2010JC006819
Serafin, K. A., Ruggiero, P., Barnard, P. L., & Stockdon, H. F. (2019). The influence of shelf bathymetry and beach topography on extreme total water levels: Linking large-scale changes of the wave climate to local coastal hazards. *Coastal Engineering*, *150*, 1–17. https://doi.org/10.1016/j.coastaleng.2019.03.012
Serafin, K. A., Ruggiero, P., & Stockdon, H. F. (2017). The relative contribution of waves, tides, and non-tidal residuals to extreme total water levels on US West Coast sandy beaches. *Geophysical Research Letters*, *44*, 1839–1847. https://doi.org/10.1002/2016GL071020
Slangen, A. B., Meyssignac, B., Agosta, C., Champollion, N., Church, J. A., Fettweis, X., et al. (2017). Evaluating model simulations of twentieth-century sea level rise. Part I: Global mean sea level change. *Journal of Climate*, *30*, 8539–8563.
Slangen, A. B. A., Carson, M., Katsman, C. A., van de Wal, R. S. W., Koehl, A., Vermeersen, L. L. A., & Stammer, D. (2014). Projecting twenty-first century regional sea-level changes. *Climate Change*, *124*(1-2), 317–332. https://doi.org/10.1007/s10584-014-1080-9
Slangen, A. B. A., & van de Wal, R. S. W. (2011). An assessment of uncertainties in using volume-area modelling for computing the twenty-first century glacier contribution to sea-level change. *The Cryosphere*, *5*(3), 673–686. https://doi.org/10.5194/tc-5-673-2011
Stockdon, H. F., Holman, R. A., Howd, P. A., & Sallenger, A. H. (2006). Empirical parameterization of setup, swash, and runup. *Coastal Engineering*, *53*(7), 573–588. https://doi.org/10.1016/j.coastaleng.2005.12.005
Stockdon, H. F., Sallenger, A. H., Holman, R. A., & Howd, P. A. (2007). A simple model for the spatially-variable coastal response to hurricanes. *Marine Geology*, *238*(1-4), 1–20. https://doi.org/10.1016/j.margeo.2006.11.004
Stockdon, H. F., Thompson, D. M., Plant, N. G., & Long, J. W. (2014). Evaluation of wave runup predictions from numerical and parametric models. *Coastal Engineering*, *92*, 1–11. https://doi.org/10.1016/j.coastaleng.2014.06.004
Sunamura, T. (1984). Quantitative predictions of beach-face slopes. *Geological Society of America Bulletin*, *95*(2), 242–245. https://doi.org/10.1130/0016-7606(1984)95<242:QPOBS>2.0.CO;2
Taylor, K. E., Stouffer, R. J., & Meehl, G. A. (2012). An overview of CMIP5 and the experiment design. *Bulletin of the American Meteorological Society*, *93*(4), 485–498. https://doi.org/10.1175/BAMS-D-11-00094.1
Vitousek, S., Barnard, P. L., Fletcher, C. H., Frazer, N., Erikson, L., & Storlazzi, C. D. (2017). Doubling of coastal flooding frequency within decades due to sea-level rise. *Nature*, *7*, 1399.
Vousdoukas, M. I., Mentaschi, L., Voukouvalas, E., Bianchi, A., Dottori, F., & Feyen, L. (2018). Climatic and socioeconomic controls of future coastal flood risk in Europe. *Nature Climate Change*, *8*(9), 776–780. https://doi.org/10.1038/s41558-018-0260-4
Vousdoukas, M. I., Mentaschi, L., Voukouvalas, E., Verlaan, M., & Feyen, L. (2017). Extreme Sea levels on the rise along Europe's coasts. *Earth's Future*, *5*(3), 304–323. https://doi.org/10.1002/2016EF000505
Vousdoukas, M. I., Mentaschi, L., Voukouvalas, E., Verlaan, M., Jevrejeva, S., Jackson, L. P., & Feyen, L. (2018). Global probabilistic projections of extreme sea levels show intensification of coastal flood hazard. *Nature Communications*, *9*(1), 2360. https://doi.org/10.1038/s41467-018-04692-w
Vousdoukas, M. I., Voukouvalas, E., Mentaschi, L., Dottori, F., Giardino, A., Bouziotas, D., et al. (2016). Developments in large-scale coastal flood hazard mapping. *Natural Hazards and Earth System Sciences*, *16*(8), 1841–1853. https://doi.org/10.5194/nhess-16-1841-2016
Vousdoukas, M. I., Wziatek, D., & Almeida, L. P. (2012). Coastal vulnerability assessment based on video wave run- up observations at a mesotidal, steep-sloped beach. *Ocean Dynamics*, *62*(1), 123–137. https://doi.org/10.1007/s10236-011-0480-x
Wada, Y., van Beek, L. P. H., Sperna Weiland, F. C., Chao, B. F., Wu, Y.-H., & Bierkens, M. F. P. (2012). Past and future contribution of global groundwater depletion to sea-level rise. *Geophysical Research Letters*, *39*, L09402. https://doi.org/10.1029/2012GL051230
Wadey, M., Brown, S., Nicholls, R. J., & Haigh, I. (2017). Coastal flooding in the Maldives: An assessment of historic events and their implications. *Natural Hazards*, *89*(1), 131–159. https://doi.org/10.1007/s11069-017-2957-5
Wahl, T., Haigh, I. D., Nicholls, R. J., Arns, A., Dangendorf, S., Hinkel, J., & Slangen, A. B. A. (2017). Understanding extreme sea levels for broad-scale coastal impact and adaptation analysis. *Nature Communications*, *8*(1), 16,075. https://doi.org/10.1038/ncomms16075
Wandres, M., Pattiaratchi, C., & Hemer, M. A. (2017). Projected changes of the southwest Australian wave climate under two atmospheric greenhouse gas concentration pathways. *Ocean Modelling*, *117*, 70–87. https://doi.org/10.1016/j.ocemod.2017.08.002
Wang, X. L., Feng, Y., & Swail, V. R. (2014). Changes in global ocean wave heights as projected using multimodel CMIP5 simulations. *Geophysical Research Letters*, *41*, 1026–1034. https://doi.org/10.1002/2013GL058650
Wong, P. P., Losada, I. J., Gattuso, J.-P., Hinkel, J., Khattabi, A., McInnes, K. L., et al. (2014). Coastal systems and low-lying areas. In C. B. Field, et al. (Eds.), *Climate Change 2014: Impacts, Adaptation, and Vulnerability. Part A: Global and Sectoral Aspects. Contribution of*

Working Group II to the Fifth Assessment Report of the Intergovernmental Panel on Climate Change (pp. 361–409). Cambridge, UK and New York, NY: Cambridge University Press.

Woodworth, P., Melet, A., Marcos, M., Ray, R. D., Wöppelmann, G., Sasaki, Y. N., et al. (2019). Forcing factors affecting sea level changes at the coast. *Surveys in Geophysics*, *40*(6), 1351–1397. https://doi.org/10.1007/s10712-019-09531-1

Wright, L. D., & Short, A. D. (1984). Morphodynamic and variability of surf zones and beaches: A synthesis. *Marine Geology*, *56*(1-4), 93–118. https://doi.org/10.1016/0025-3227(84)90008-2

Wunsch, C., & Stammer, D. (1997). Atmospheric loading and the oceanic "inverted barometer" effect. *Reviews of Geophysics*, *35*(1), 79–107. https://doi.org/10.1029/96RG03037

Young, I. R., & Ribal, A. (2019). Multiplatform evaluation of global trends in wind speed and wave height. *Science*, *364*(6440), 548–552. https://doi.org/10.1126/science.aav9527